Title: Florigen Activation Complex Dynamics and SVP-Mediated Repression Orchestrate Temperature-Regulated Flowering in Saffron

Authors: Diksha Kalia[1, 2], Joel Jose-Santhi[1, 2], Firdous Rasool Sheikh[1, 2], and Rajesh Kumar Singh[1, 2, *]

Affiliations:

1. Plant Adaptation and Developmental Biology Lab, Department of Biotechnology, CSIR-Institute of Himalayan Bioresource Technology, Palampur, H.P., India-176061
2. Academy of Scientific and Innovative Research (AcSIR), Ghaziabad, 201002, India

Author Details:

Diksha Kalia, email: dikshakalia47@gmail.com,

Joel Jose -Santhi, email: joeljosesanthi@gmail.com,

Firdous Rasool Sheikh, email: sheikhfirdous191@gmail.com,

Rajesh Kumar Singh: *Corresponding Author, email: rajeshsingh@ihbt.res.in, ORCID Id: 0000-0001-7831-7946

Abstract

Saffron, a high-value spice cultivated worldwide for its therapeutic and culinary uses, is a sterile triploid species, rendering conventional breeding approaches ineffective. This limitation underscores the need for molecular and biotechnological strategies for its genetic improvement. Flowering, a key determinant of saffron yield, is strongly influenced by temperature; however, the genetic regulatory networks underlying this process remain poorly understood. Our study identifies key regulators of saffron's flowering, focusing on the Florigen Activation Complex (FAC) components: *FLOWERING LOCUS T* (FT), bZIP transcription factor FD, and *TERMINAL FLOWER*-1 (TFL-1), and demonstrate their temperature-dependent roles in floral regulation. Spatiotemporal expression analyses suggested that *CsatFT3* and *CsatFD2*, expressed in the floral meristem promote floral induction, while *CsatTFL1*-3 acts as a floral repressor. Protein interaction studies showed that CsatFT3 and CsatTFL1-3 compete for binding to CsatFD2, and their balance modulates floral induction. Functional validation in Arabidopsis and Saffron confirmed these findings. Furthermore, we identified *CsatSVP2*, an ortholog of *SHORT VEGETATIVE PHASE* (SVP), as a low temperature-responsive repressor that directly binds the CsatFT3

promoter to inhibit its expression. Together, these findings enhance our understanding of temperature mediated floral induction in saffron and provide insights and lay the groundwork for genetic interventions to enhance yield under variable temperature conditions.

Keywords: Florigen activation complex (FAC), Flowering locus T(FT), bZIP transcription factor-FD, *TFL1*, Geophytes, Thermoresponsive, Thermoperiodic, Floral induction, Phosphatidyl Ethanolamine Binding Protein (PEBP), VIGS,

Introduction

Saffron (*Crocus sativus* L.) is a sterile, clonally propagated, autotriploid geophytic monocot cultivated for its highly valued dried stigmas, which constitute the world's most expensive spice. While the stigmas are the primary edible and culinary component, other parts of the saffron plant also have diverse applications, including uses in agriculture, traditional medicine, and as a natural colouring agent, making the entire flower economically valuable (Ahrazem et al., 2015). Saffron has been predominantly cultivated for centuries in select regions such as Iran, India, Greece, Italy, Afghanistan, Morocco, Spain, and various Mediterranean basins (Cardone et al., 2020). Flowering is the key determinant of saffron's crop productivity, and this critical phase is increasingly influenced by environmental changes. As a thermoperiodic plant, saffron's flowering is primarily regulated by temperature. During the warm summer months, the transition from vegetative to reproductive growth occurs underground, with floral bud emergence only triggered by exposure to cooler temperatures (Molina et al., 2005a). This biphasic thermal requirement consists of an induction phase at warm temperatures lasting 50–150 days, followed by an emergence phase under cooler conditions, a pattern that has been well documented (Jose-Santhi et al., 2023; Molina et al., 2005a). The inappropriate temperature during the flowering transition leads to flower atrophy or no flower, causing yield loss (Wang et al., 2021). Saffron corms can sense the temperature change and modify the response accordingly (Molina et al., 2005b). Thus, there exists a thermoresponsive regulation of flowering in saffron which is still not well studied at the molecular level.

Flowering is a key transition in the angiosperm life cycle, marking the shift from vegetative to reproductive growth and representing a tightly regulated process vital for survival. This process is orchestrated by a complex network of environmental cues,

internal signalling pathways, hormonal regulation, and genetic programs that together ensure flowering occurs under optimal conditions (Zik and Irish, 2003). Key environmental pathways influencing flowering include photoperiod, ambient temperature, light quality, vernalization, and gibberellin signalling. These pathways operate in coordination with endogenous factors along with plant age and nutritional status, allowing plants to synchronize reproduction with favourable environmental windows (Andrés and Coupland, 2012; Freytes et al., 2021; Pyo et al., 2014; Srikanth and Schmid, 2011). Extensive studies in model organisms such as Arabidopsis thaliana have elucidated major regulatory components of flowering (Kinoshita and Richter, 2020). Central to this regulation are floral integrator genes, particularly *FLOWERING LOCUS T* (FT) a member of the phosphatidylethanolamine-binding protein (PEBP) family. FT functions to promote flowering by forming the Florigen Activation Complex (FAC), which includes FD-like bZIP transcription factors and the florigen receptor 14-3-3 protein (Abe et al., 2005; Taoka et al., 2013). This complex activates floral meristem identity genes such as *LEAFY* and *APETALA1*, initiating floral development (Putterill et al., 2004; Simon et al., 1996; Wigge et al., 2005). In contrast, *TERMINAL FLOWER 1* (TFL1), another PEBP family member, acts antagonistically to repress flowering (Wickland and Hanzawa, 2015). Members of the FD family are key interaction partners of the PEBP family, playing roles in both promoting and repressing meristem differentiation, depending on their specific interacting partners (Zhu et al., 2020). Concurrently, the flowering program suppresses negative regulators, including *FLOWERING LOCUS C* (FLC), and *SHORT VEGETATIVE PHASE* (SVP), which are crucial for ensuring a proper transition from the vegetative to the reproductive phase mainly regulated by temperature (Bowman et al., 2012; Turck et al., 2008). Temperature-dependent flowering has been widely studied, with FT-like genes playing a central role (Capovilla et al., 2015) . Upstream regulators include MADS-domain transcription factors such as SVP and FLC, which modulate flowering by forming complexes and repressing FT expression via direct binding to its promoter (Balasubramanian et al., 2006; Gu et al., 2013; Lee et al., 2007). However, the thermoresponsive pathway governing floral induction in saffron remains largely unexplored.

In contrast to annuals, the regulation of flowering in perennial geophytes involves modified or additional mechanisms to accommodate their extended life cycles, periods of dormancy and dual reproduction (Khosa et al., 2021) . This has been observed in

species like *Narcissus tazetta* (Noy-Porat et al., 2013), tulip (Tulipa spp.) (Leeggangers et al., 2017b), and saffron (Molina et al., 2005a), where floral induction occurs even in the absence of leaves. In these species, flowering is thought to be mediated directly at the meristem level, independent of traditional photoperiod or vernalization cues. Instead, ambient temperature plays a dominant role in determining flowering time. These observations highlight the need to identify the specific genes and mechanisms that govern flowering in geophytic perennials. Over evolutionary time, the molecular mechanisms controlling flowering have grown increasingly complex, involving intricate interactions between floral regulator genes and their transcription factor partners, which form regulatory complexes (Wickland and Hanzawa, 2015) . Gene duplication and neofunctionalization have contributed to the diversification of these regulatory genes. Both *FT* and *TFL1,* the central regulators of flowering, have undergone gene duplication events in various lineages, leading to paralogs with distinct functions that promote or inhibit flowering (Jin et al., 2021) . This evolutionary diversification is evident across many species. In geophytes, for instance, members of the PEBP gene family have extended their functions beyond flowering to include the formation of underground storage organs, contributing to both sexual and asexual reproduction (Khosa et al., 2021). In species like potato, tulip, and others, gene duplication has led to distinct roles in flowering, vegetative growth, and tuber or bulb formation (Bellinazzo et al., 2025; Jing et al., 2023; Navarro et al., 2011). Similar divergence has been observed in onion (Allium cepa), sugar beet (Beta vulgaris), and hybrid aspen, demonstrating the complexity of flowering regulation in perennials (Hsu et al., 2011; Lee et al., 2013b; Pin et al., 2010). Beyond the PEBP gene family, functional diversification is seen in related pathways. In hybrid aspen, two FD homologs, *FDL1* and *FDL2*, regulate seasonal growth differently (Tylewicz et al., 2015). In rice, *OsFD2* contributes to leaf development while *OsFD1* regulates flowering (Tsuji et al., 2013). FD-like transcription factors can have dual roles, promoting or repressing flowering depending on their partners. For instance, *CmFDa* in Chrysanthemum morifolium represses flowering through epigenetic regulation (Xue et al., 2025). These examples highlight the evolutionary plasticity of flowering networks and the importance of species-specific regulatory mechanisms.

Saffron, due to its sterile nature and extremely limited genetic diversity, is not amenable to conventional breeding approaches, which hinders efforts to develop climate-resilient, high-yielding, and stress-tolerant varieties. As a result, there have

been no significant advancements in improving saffron's adaptability to climate change, making its cultivation increasingly vulnerable to environmental fluctuations. Consequently, only biotechnological interventions can be employed to introduce desirable traits. Despite its economic and agricultural importance, research on the molecular regulation of flowering in saffron remains limited. Most existing studies have focused on temperature effects on flowering physiology (Molina et al., 2005a; Wang et al., 2021), and while several flowering-related genes have been identified through transcriptomic and genomic analyses (Hu et al., 2020; Kalia et al., 2022; Renau-Morata et al., 2021; Singh et al., 2023; Tsaftaris et al., 2013), these remain largely descriptive and lack functional validation. Expression profiling has indicated the involvement of multiple *FT* and *TFL1* homologs in saffron flowering (Kalia et al., 2022; Renau-Morata et al., 2021; Tsaftaris et al., 2013), yet no functional characterization of these genes has been reported. To fill this gap, we present a comprehensive molecular framework for temperature-dependent floral induction in saffron—a geophytic monocot with a unique flowering phenotype. By integrating gene expression profiling, heterologous functional assays, protein–protein interaction studies, promoter binding analyses, and virus-induced gene silencing, we identify key regulatory components that mediate the floral transition in response to ambient temperature. Overall, these findings advance our understanding of temperature-mediated flowering in saffron and provide a foundation for genetic interventions aimed at improving yield under fluctuating environmental conditions

Methods

Plant materials and growth conditions

Saffron corms *(Crocus sativus* L.) were grown under controlled conditions at CSIR-IHBT, and samples were collected monthly from January to September, covering both the vegetative growth and flowering phases (Jose-Santhi et al., 2023; Kalia et al., 2022). To analyze gene expression patterns, apical buds, axillary buds, and corm tissues were harvested across this period, with three biological replicates per time point, each comprising pooled tissue from ten individual corms. For RT-qPCR analysis, apical buds, axillary bud, corm tissue collected during the vegetative and flowering stages were used, with detailed methods and results provided in the Supplementary Information.

169 ViGS experiments were conducted using corms grown under the same controlled
170 conditions as described earlier. Corms with high flowering competency (weighing >10
171 g) were selected for the silencing of *CsatFT3* and *CsatFD2*. To investigate the role of
172 *CsatSVP2*, two experimental conditions were used: (i) standard growth conditions, and
173 (ii) a temperature-sensitive treatment in which corms were incubated at 8 °C during
174 the flowering phase to assess temperature-dependent gene regulation. For silencing
175 of *CsatTFL1-3/CEN1*, corms with lower flowering competency (weighing 7–9 g) were
176 utilized.
177 *Arabidopsis thaliana* (Col-0) was used as the wild-type background for transformation
178 experiments, and the ft1 mutant in the Ler background was used for functional
179 complementation of CsatFT3. *Nicotiana benthamiana* was used for transient
180 expression assays. Arabidopsis seeds were surface-sterilized with 4% sodium
181 hypochlorite and germinated on half-strength Murashige and Skoog (MS) medium. To
182 synchronize germination, seeds were stratified at 4°C for two days before being
183 transferred to a soil mixture of peat, vermiculite, and perlite (2:1:1). All plants were
184 cultivated in controlled growth chambers under long-day conditions (16 h light/8 h
185 dark) at 22°C for Arabidopsis and 25°C for *Nicotiana benthamiana*.
186
187 **RNA isolation and expression analysis by RT-qPCR**
188 Total RNA was isolated from saffron apical buds, axillary buds, corm tissues, and
189 Arabidopsis using the Plant Total RNA Isolation Kit (Sigma-Aldrich), according to the
190 manufacturer's protocol. For each sample, 1 µg of total RNA was used to synthesize
191 cDNA. Reverse transcription was performed using the RevertAid cDNA Synthesis Kit.
192 The transcript level of each gene was quantified by quantitative real-time PCR (q-PCR)
193 using gene-specific primers (Supplementary Table 1), generated by SnapGene
194 Viewer 5.3.1 software (version 0.4.0) using the System (BioRad CFX Opus Real time
195 PCR). Each expression analysis included three biological replicates, with each
196 replicate derived from pooled tissue of ten individual corms. RT-qPCR results are
197 presented as the mean ± standard error (SEM) of three technical replicates per
198 biological sample.
199
200 **Sequence alignments and phylogenetic analysis**
201 Protein sequences were aligned using the ClustalW algorithm with default parameters
202 to generate high-quality multiple sequence alignments. Visualization of the alignments

203 was performed using ESPript 3.x (Robert & Gouet, 2014) to highlight conserved
204 regions and structural features. The aligned sequences were exported in Newick
205 (.nwk) format for phylogenetic analysis. Phylogenetic tree construction was carried out
206 using the "build" function of ETE3 v3.1.3 (Huerta-Cepas et al., 2016), implemented via
207 the GenomeNet platform (https://www.genome.jp/tools/ete/). FastTree v2.1.8 (Price et
208 al., 2010) was used with default settings to infer approximately maximum-likelihood
209 phylogenetic trees.
210

211 **Plant transformation**

212 To generate Arabidopsis transgenic lines, full-length coding sequences (CDS) of the
213 target genes were amplified and first cloned into the pENTR entry vector using
214 Gateway® cloning technology. Subsequently, LR recombination was performed to
215 transfer the CDS into the destination vectors pK2GW7 (for overexpression analysis),
216 under the control of the Cauliflower Mosaic Virus (CaMV) 35S promoter. The resulting
217 constructs included 35S::*CsatFD1*, 35S::*CsatFD2*, 35S::*CsatFD3*, 35S::*CsatFT3*,
218 35S::*CsatTFL1-1*, 35S::*CsatTFL1-2*, 35S::*CsatTFL1-3*, 35S::*CsatSVP1*, and
219 35S::*CsatSVP2*. Primer sequences used for vector construction are provided in the
220 supplementary table 1 file. The final recombinant plasmids were introduced into
221 *Arabidopsis thaliana* (Col-0) via Agrobacterium tumefaciens strain GV3101 using the
222 floral dip transformation method. Transgenic seeds were harvested individually and
223 screened based on the appropriate selection marker. Homozygous T3 lines were
224 identified and used for further phenotypic characterization. Flowering time was
225 recorded as the number of days from germination to the emergence of the first floral
226 bud.
227

228 **Yeast one hybrid (Y1H) assay**

229 To examine the binding of CsatSVP2 to the CsatFT3 promoter, yeast one-hybrid (Y1H)
230 assays were conducted using the Matchmaker® Gold Yeast One-Hybrid System Kit
231 (Clontech). Promoter fragments of CsatFT3 containing the core CArG-box motif were
232 cloned into the pAbAi vector. The resulting recombinant pAbAi-promoter plasmids
233 were linearized with BstBI (NEB) and integrated into the genome of the Y1HGold yeast
234 strain. Transformants were selected on synthetic dextrose (SD) medium lacking uracil
235 (SD/-Ura). The coding sequence of CsatSVP2 was amplified and inserted into the
236 pGADT7-AD vector. The recombinant pGADT7-AD constructs were then introduced

237 into the Y1HGold strains containing the integrated CsatFT3 promoter. Protein–DNA
238 interaction was assessed by culturing the transformed yeast on SD medium lacking
239 leucine (SD/-Leu) and supplemented with Aureobasidin A (AbA) at a minimal inhibitory
240 concentration of 150 ng/mL for four days. Primer sequences used for cloning are
241 provided in Supplementary Table 1.
242
243 **Histochemical localization of GUS activity**
244 GUS activity was performed using the histochemical staining protocol described by
245 Jefferson(Jefferson et al., 1987). Transgenic *Arabidopsis thaliana* lines with
246 *ProCsatFT3::GUS* construct were incubated in a staining solution composed of 50 mM
247 sodium phosphate buffer (pH 7.2), 2.0 mM potassium ferricyanide [$K_3Fe(CN)_6$], 2.0
248 mM potassium ferrocyanide [$K_4Fe(CN)_6$], 0.1% (v/v) and 1.0 mg/mL X-Gluc (5-bromo-
249 4-chloro-3-indolyl-β-D-glucuronide). Samples were incubated at 37 °C for 5 hours to
250 allow GUS expression to develop. Following staining, tissues were cleared with 70%
251 (v/v) ethanol to remove chlorophyll and enhance contrast, then examined under a
252 stereo microscope (ZEISS Stemi 508). To validate GUS expression patterns, at least
253 ten independent transgenic lines were screened for the construct. Plants from three
254 confirmed GUS-positive lines were selected for detailed expression analysis at various
255 developmental stages, including 7, 14, and 21 days after germination (DAG),
256 inflorescence emergence, flowering, and silique formation. For the flowering and
257 silique stages, staining was performed on aerial tissues from soil-grown plants
258
259 **Yeast two-hybrid (Y2H) assays**
260 Yeast two-hybrid assays were conducted following the manufacturer's protocol using
261 the Matchmaker™ Two-Hybrid System (Clontech). The coding sequences of
262 CsatFD1, CsatFD2, and CsatFD3 were cloned into the bait vector pGBKT7, whereas
263 those of CsatFT3, CsatTFL1-1, CsatTFL1-2, and CsatTFL1-3 were inserted into the
264 prey vector pGADT7. The primers used for amplification are provided below. Bait and
265 prey plasmids were co-transformed into the Y2HGold yeast strain and cultured on
266 synthetic dextrose (SD) medium lacking tryptophan (SD/-Trp) and leucine (SD/-Leu)
267 for 3–5 days at 30°C. Protein-protein interactions were assessed by selecting colonies
268 on SD medium lacking Trp, Leu, and histidine (SD/-Trp/-Leu/-His).
269
270 **Bimolecular fluorescence complementation (BiFC)**

271 The coding sequences of *CsatFD1*, *CsatFD2*, *CsatFD3* Cloned into YFP C-terminal
272 (YFPC) and *CsatFT3*, *CsatTFL1-1*, *CsatTFL1-2*, *CsatTFL1-3* were cloned into the
273 YFP N-terminal (YFPN) vectors. Primer sequences used for vector construction are
274 provided in the supplementary table 1. These constructs were then introduced into
275 Agrobacterium tumefaciens strain GV3101 for transient expression in 5-week-old
276 *Nicotiana benthamiana* leaves. After co-infiltration for 48 hours, fluorescence was
277 imaged using a confocal laser scanning microscope (Leica TCS SP5, Germany).YFP
278 fluorescence was excited at 514 nm, with emission detected between 522 and 560
279 nm.
280
281 **Firefly Complementation Assay**
282 The full-length coding sequences (CDSs) of CsatFT3, CsatTFL1-3, and CsatFD2 were
283 cloned into the pCAMBIA1300-nLUC and pCAMBIA1300-cLUC vectors, respectively,
284 and introduced into Agrobacterium tumefaciens strain GV3101. Various combinations
285 were co-infiltrated into Nicotiana benthamiana leaves. The infiltrated plants were
286 incubated at 22 °C for two days. Prior to LUC activity detection, the leaves were
287 sprayed with 1 mM D-luciferin (Potassium Salt, BioVision) and incubated in the dark
288 for 8 minutes to eliminate background fluorescence. Fluorescence was detected using
289 a cooled CCD camera system (Bio-Rad Chemi Doc). Relative LUC intensity was
290 quantified using ImageJ software. Statistical analysis was performed using one-way
291 ANOVA, and significance was assessed using the Compact Letter Display (CLD)
292 method to indicate differences at a significant p-value level. Primer sequences used
293 in these assays are provided in Supplementary Table 1.
294
295 **Genome walker library for promoter amplification**
296 The 5′ upstream region of the CsatFT3 gene from Crocus sativus was obtained using
297 the Genome Walker™ kit (Clontech, USA). Genomic DNA was extracted from leaf
298 tissue following the protocol provided with the QIAGEN DNA isolation kit, then
299 digested with two blunt-end restriction enzymes, DraI and EcoRV, and further ligated
300 with adapters, to generate Genome Walker libraries. Gene-specific primers (GSPs),
301 designed based on the CsatFT3 cDNA sequence, were used alongside adaptor
302 primers from the kit to carry out primary and nested PCR amplifications as listed in
303 Supplementary Table 1. The amplified PCR products were resolved on a 1% (w/v)
304 agarose gel, purified, and cloned into the pGEM-T Easy vector (Promega, USA) for

305 sequencing. The resulting CsatFT3 promoter sequence was analyzed using the
306 PlantCARE database (Lescot et al., 2002) to identify potential cis-regulatory elements
307 involved in transcriptional regulation.
308
309 **Virus-induced gene silencing (VIGS)**
310 Virus-induced gene silencing (VIGS) was carried out following the protocol established
311 in lab (Kalia et al., 2024). Gene-specific fragments were amplified for *CsatFT3* (300
312 bp, flanked by EcoRI sites), *CsatFD2* (292 bp, flanked by BamHI sites), *CsatTFL1-3*
313 (302 bp, containing both EcoRI and BamHI sites), and *CsatSVP2* (318 bp, with
314 EcoR1and BamH1 sites) restriction sites at both termini. These fragments were cloned
315 into the pTRV2 vector to generate the constructs. Agrobacterium-mediated infiltration
316 was performed as previously described (Kalia et al., 2024). To confirm gene silencing,
317 transcript levels of *CsatFT3*, *CsatFD2*, *CsatTFL1-3*, and *CsatSVP2* were quantified by
318 RT-qPCR in apical buds collected at the floral induction stage. Phenotypic analysis of
319 flower development was conducted when floral buds reached the floral emergence
320 stage. Primer sequences used for the VIGS assay are listed in Supplementary table
321 1.
322
323 **Luciferase assay**
324 To investigate the regulatory effect of *CsatSVP2* on the *CsatFT3* promoter, a
325 luciferase reporter assay was conducted in *Nicotiana benthamiana* leaves. Promoter
326 sequences of *CsatFT3* were cloned into the Gateway-compatible vector pGWB435
327 (Invitrogen) upstream of the luciferase (Luc) reporter gene. Three promoter constructs
328 were generated: (i) the full-length promoter (FL), (ii) a truncated fragment containing
329 the CArG motif(T1), and (iii) a truncated fragment lacking the CArG motif (T2). The
330 *CsatSVP2* coding sequence was separately cloned into pGWB402 under the control
331 of the CaMV35S promoter to serve as an effector. Control treatments included empty
332 vectors (pGWB435 and pGWB402) as a negative control, and *ProCsatFT3*::Luc alone
333 as a positive control. Constructs were introduced into the *Agrobacterium tumefaciens*
334 strain GV3101 and co-infiltrated into *Nicotiana benthamiana* leaves. Each leaf was
335 divided into four quadrants to enable side-by-side comparisons of different treatments
336 within the same biological context. Luciferase activity was visualized and quantified
337 using ImageJ software. The experiment was repeated independently at least three
338 times in separate leaves to ensure reproducibility. One-way ANOVA was used for

339 statistical analysis, and differences among treatments were determined using
340 Compact Letter Display (CLD) to indicate statistically significant differences ($p < 0.05$).
341
342 **Statistical analyses**
343 All statistical analyses were conducted using GraphPad Prism version 10 for Windows
344 (GraphPad Software, Boston, MA, USA; www.graphpad.com). One-way ANOVA
345 followed by Tukey's Honest Significant Difference (HSD) test was applied for multiple
346 comparisons. Statistically significant differences between groups at $p < 0.05$ are
347 indicated by different letters, as determined by Compact Letter Display (CLD).Two-
348 way ANOVA to assess the effects of temperature, month, and their interaction,
349 followed by Sidak's multiple comparisons test and Student's t-test for one-to-one
350 comparison. (*: $p<0.05$; **: $p<0.01$***: $p<0.001$) (****: $p<0.0001$).
351
352 **Results:**
353 **CsatFT3 functions as a temperature-sensitive regulator of floral induction in**
354 **saffron**
355 Our previous work identified several PEBP family genes implicated in flowering
356 regulation in saffron, with *CsatFT3* emerging as a potential key regulator of floral
357 induction (Kalia et al., 2023). However, that study was limited to spatial and temporal
358 expression profiling during the reproductive phase transition. To further elucidate the
359 functional role of *CsatFT3*, we investigated its expression dynamics across vegetative
360 and reproductive phases in saffron apical buds. We found that *CsatFT3* is specifically
361 expressed during the reproductive phase, with transcript accumulation coinciding with
362 the floral induction stage (Figure 1A, Supplementary Figure 1). In contrast, its
363 expression was barely detectable in apices of newly developing corms and during the
364 vegetative phase in winter. Given that low temperatures are known to suppress floral
365 induction in saffron (Jose-Santhi et al., 2023), we next assessed *CsatFT3* expression
366 in apical buds of corms stored under low (8°C) and ambient (25°C) temperature
367 conditions following the vegetative phase. Consistent with a temperature-responsive
368 role, *CsatFT3* transcript levels were markedly reduced in corms stored at 8°C
369 compared to those maintained at 25°C (Figure 1B).
370 To further investigate tissue- and temperature-specific expression of the *CsatFT3*
371 gene, we isolated a 1.2 kb fragment of the *CsatFT3* promoter (Supplementary figure
372 2) that contains several core, distal, and proximal promoter elements and constructed

373 a promoter-GUS fusion construct. GUS-driven transcription reporter lines of *CsatFT3*
374 displayed meristem and flower-specific expression in Arabidopsis, consistent with our
375 spatiotemporal expression profiling in saffron (Figure 1C and Supplementary figure 3).
376 Furthermore, these *ProCsatFT3::GUS* fusion lines demonstrated temperature-
377 sensitive regulation, with expression gradually decreasing as the temperature was
378 lowered, in line with our previous findings that low temperatures suppress the
379 expression of *CsatFT3* (Figure 1D). At low temperatures (4°C), GUS activity was
380 nearly undetectable, indicating a significant suppression of expression under cold
381 conditions. These findings reinforce the role of *CsatFT3* in temperature-sensitive
382 flowering regulation in saffron and suggest that its expression is activated under the
383 relatively high-temperature conditions that promote floral induction.
384 To functionally validate the role of *CsatFT3* in floral regulation, we ectopically
385 expressed *CsatFT3* in Arabidopsis Col-0 and complemented the late-flowering ft-10
386 mutant (Ler-0). Overexpression in Col-0 resulted in a significant early-flowering
387 phenotype (Figure 1E–G), while ft-10 plants transformed with *CsatFT3* exhibited
388 restored or even earlier flowering compared to wild-type (Figure 1H–J). These results
389 confirm that *CsatFT3* is functionally conserved and capable of promoting flowering in
390 a heterologous system. Following confirmation of CsatFT3's involvement in floral
391 induction and flowering, finally, to evaluate the role of *CsatFT3* in its native we
392 performed Virus-Induced Gene Silencing (VIGS) of *CsatFT3* in saffron corms and
393 monitored flowering. Silencing of *CsatFT3* led to a significant reduction in its transcript
394 levels in apical buds (Figure 1K) and was accompanied by a marked decrease in
395 flowering percentage compared to TRV2 mock-infected controls (Figure 1L–M). No
396 significant decrease of *CsatFT1* and *CsatFT2* was observed in TRV2-silenced
397 CsatFT3 corms (Supplementary Figure 4). Together, these findings establish CsatFT3
398 as a temperature-sensitive floral inducer in saffron, functioning as a key regulatory
399 component during the transition from vegetative to reproductive growth.
400

401 **Identification of florigen activation complex component FD, involved in**
402 **flowering induction in saffron**

403 *FT* like genes requires interaction with bZIP transcription factor-*FD* to form FT-FD
404 complex that directly activates the floral meristem identity genes. Thus, to identify the
405 FD like genes involved in floral induction of saffron we have cloned full length cDNAs
406 for three FD-like genes (*CsatFD1*, *CsatFD2* and *CsatFD3*), which encodes for 197,

407 215 and 245 aa of proteins respectively. All the three FDs are similar to FD proteins
408 from other plants and contains the conserved basic region, Leucine zipper region and
409 the functionally important conserved threonine (T)/SAP motif at the C terminus
410 (Supplementary Figure 5A). Phylogeny aligns CsatFD's with monocot FDs with
411 Asparagus officinalis as the nearest family member (Supplementary Figure 5B).
412 We next investigated the expression profiles of the three saffron *FD* genes during the
413 vegetative and flowering induction stages. Interestingly, the expression of *CsatFD2*
414 coincided with the floral induction stage, whereas *CsatFD3* showed higher expression
415 at later stages of sprouting, specifically in July, when floral differentiation and
416 vegetative growth begin (Figure 2 A). In contrast, *CsatFD1* was expressed at relatively
417 stable levels throughout flower initiation and the vegetative phase, but its expression
418 was generally lower compared to *CsatFD2* and *CsatFD3*. In saffron, the apical bud
419 gives rise to the flower, while the axillary buds contribute only to vegetative growth,
420 thereby distinguishing the reproductive meristem from the vegetative meristems (Kalia
421 et al., 2022). Notably, *CsatFD2* was predominantly expressed in apical buds and
422 flower tissues, indicating a primary role in flowering (Figure 2B, C). Additionally,
423 *CsatFD2* showed comparatively higher expression in flower tissues compared to the
424 other two FD genes (Figure 2C). We also examined the temperature-sensitive
425 expression of these genes in corms stored at low and ambient high temperatures. Our
426 results showed that only *CsatFD2* expression was significantly downregulated at low
427 temperatures (Figure 2D), while the expression of *CsatFD1* and *CsatFD3* did not
428 exhibit a similar pattern (Supplementary Figure 6A). Interestingly, *CsatFD3* was highly
429 expressed in corms stored at low temperatures (Supplementary Figure 6B).
430 Next, we examined the effect of ectopic expression of the saffron *FD* genes in
431 Arabidopsis. Ectopic expression of *CsatFD2* can only induce early flowering in
432 Arabidopsis, whereas there was no significant phenotypic change observed in
433 *CsatFD1* and *CsatFD3* expressing Arabidopsis plants (Figure 2E). These findings
434 were further supported by measurements of days to flowering and the number of
435 rosette leaves in the Arabidopsis transformants (Figures 2F-K). These results further
436 suggest that *CsatFD2* may be the primary gene involved in flowering regulation in
437 saffron. To confirm the role of *CsatFD2* during floral induction, we silenced the gene
438 using Virus-Induced Gene Silencing (VIGS) in flower-competent saffron corms.
439 Compared to the TRV2 control, silencing of *CsatFD2* resulted in a reduction in flower
440 formation and overall flowering percentage (Figure 2L). VIGS silencing of CsatFD2

441 also led to a significant decrease in its transcript levels (Figure 2M), but did not affect
442 the expression of *CsatFD1* and *CsatFD3* (Supplementary Figure 7 A and B). These
443 results suggest that *CsatFD2* is a key component of the Floral Activator Complex
444 (FAC) involved in floral induction in saffron.
445
446 **TFL1-3/CEN1 is a newly identified negative regulator of flowering induction in**
447 **saffron**
448 In our previous study (Kalia et al., 2023), we identified two homologs of *TFL-1*/*CEN*,
449 named Csat*TFL1-1* and Csat*TFL1-2*, and through spatio-temporal expression
450 profiling, we proposed that TFL1-2 may play a role in determining flowering
451 competency in saffron (Supplementary figure 8A and B). However, neither of these
452 two *TFL-1* genes exhibited a temperature-sensitive response (Supplementary Figure
453 9A and B). Furthermore, ectopic expression of *CsatTFL1-1* and *CsatTFL1-2* in
454 Arabidopsis led to delayed bolting in only *CsatTFL1-2* plants compared to wild-type
455 (WT) under long-day (LD) conditions, whereas *CsatTFL1-1* transformants bolted
456 normally, similar to WT plants (Supplementary figure 10A-F). Additionally, interaction
457 studies, including BiFC and Y2H assays, did not reveal any positive interactions with
458 *CsatFD2*, our identified positive regulator of flowering (Supplementary Figure 11A and
459 B). These findings prompted us to investigate further, hypothesizing that another
460 homolog of TFL1/CEN might be involved in floral induction in saffron. Through corm
461 development studies in our lab (Jose-Santhi et al., 2023), we identified a third *TFL1*
462 homolog, which exhibited higher expression during the vegetative phase. This gene
463 shares similarities with *CsatTFL1-1* and *CsatTFL1-2*, but phylogenetic analysis
464 clustered it within the CEN subgroup. Based on this, we named it *CsatTFL1-3*/*CEN1*
465 (Supplementary Figure 12A and B). Like other TFL1/CEN family members, TFL1-
466 3/CEN1 contains the conserved domains characteristic of this gene family.
467 Quantitative PCR (qPCR) expression profiling revealed that *CsatTFL1-3*/*CEN1*
468 expression is elevated during the vegetative phase, with a significant decrease during
469 the reproductive phase (Figure 3A). Tissue-specific expression analysis confirmed
470 that *CsatTFL1-3*/*CEN1* is predominantly expressed in the axillary bud tissue, further
471 supporting its potential role in negatively regulating flowering (Figure 3 C and D).
472 Next, we examined the expression of *CsatTFL1-3*/*CEN1* in corms stored at low (8°C)
473 and ambient (25°C) temperatures. Interestingly, there was no reduction in *TFL1-*
474 *3*/*CEN1* expression in corms stored at low temperatures compared to those stored at

475 ambient high temperatures, suggesting that it may be regulated by temperature and
476 could play a role in temperature-mediated floral induction in saffron (Figure 3B). We
477 then performed ectopic expression of *CsatTFL1-3*/*CEN1* in *Arabidopsis thaliana* (Col-
478 0) under the control of the constitutive 35S promoter. Transgenic lines exhibited a
479 significant delay in flowering compared to wild-type plants, as evidenced by increased
480 days to bolting and a higher number of rosette leaves at flowering (Figure 3F-G).
481 These results confirm the ability of TFL1-3/CEN1 to act as a floral repressor in
482 Arabidopsis, consistent with its proposed function in saffron. Notably, ectopic
483 expression of TFL1-3/CEN1 also led to a hyper-vegetative shoot phenotype,
484 characterized by the development of an inflorescence composed of leaf primordia
485 surrounded by small, serrated leaves—a phenotype not observed in TFL1-1 or TFL1-
486 2 expressing Arabidopsis lines (Figure 3E). Finally, we performed Virus-Induced Gene
487 Silencing (VIGS) of *CsatTFL1-3*/*CEN1* in low-flower-competent saffron corms. In
488 comparison to TRV2 control plants, silencing of *CsatTFL1-3*/*CEN1* led to the formation
489 of floral structures in 7-9 g corms (classified as low-flower-competent), and these
490 flowers appeared earlier than in TRV2 controls (Figure 3G-I). Importantly, VIGS of
491 *CsatTFL1-3*/*CEN1* did not affect the transcript levels of the other two *TFL1* homologs,
492 TFL1-1 and TFL1-2 (Supplementary Figure 13 A and B), suggesting TFL1-3/CEN1
493 and not TFL1-1 or TFL1-2 could play a role in flowering in saffron. This observation
494 suggests that TFL1-3/CEN1 acts as a negative regulator of floral induction, and its
495 silencing promotes floral transition in otherwise low-flowering competence corms.
496

497 **The FT-FD-TFL complex involved in floral regulation**

498 Our earlier analyses identified *CsatFT3*, *CsatFD2*, and *CsatTFL1-3*/*CEN1* as potential
499 core components of a Floral Activator Complex (FAC) in saffron. To investigate
500 whether these proteins physically interact to form functional regulatory complexes,
501 we employed two complementary approaches: yeast two-hybrid (Y2H) assays and
502 bimolecular fluorescence complementation (BiFC) in *Nicotiana benthamiana*. In the
503 Y2H assays, the coding sequences (CDS) of the three *CsatFD* genes were cloned into
504 the pGADT7 prey vector, and co-transformed into yeast with either *CsatFT3* or
505 *CsatTFL1-3*/*CEN1* fused to the pGBKT7 bait vector. Interaction screening revealed
506 that both CsatFT3 and TFL1-3/CEN1 specifically interacted with CsatFD2, but not with
507 CsatFD1 or CsatFD3 (Figure 4 A and B). These results suggest that CsatFD2 may

508 serve as a central interacting hub for both activator (FT3) and repressor (TFL1-3)
509 proteins within the FAC.
510 We further validated these interactions by BiFC assays in *Nicotiana benthamiana*
511 leaves. YFP fluorescence was observed in nuclei of cells co-expressing the C-terminal
512 half of YFP fused to CsatFD2 (cYFP–CsatFD2) with the N-terminal half of YFP fused
513 to either CsatFT3 (nYFP–CsatFT3) or CsatTFL1-3 (nYFP–CsatTFL1-3) (Figure 4 C
514 and D). No YFP fluorescence was detected in negative controls, including co-
515 expression of cYFP–CsatFD2 with nYFP alone or cYFP alone with nYFP–CsatFT3 or
516 CsatTFL1-3. Furthermore, consistent with the Y2H results, no BiFC signal was
517 observed when CsatFT3 or TFL1-3/CEN1 were co-expressed with CsatFD1 or
518 CsatFD3 (Supplementary Figure). Together, these findings strongly support a model
519 in which CsatFD2 specifically interacts with both CsatFT3 and TFL1-3/CEN1,
520 suggesting that competitive complex formation may modulate floral transition in
521 saffron.
522 Given the antagonistic roles of CsatFT3 and CsatTFL1-3 in the regulation of flowering,
523 and their respective interactions with the transcription factor CsatFD2, it was
524 hypothesized that CsatFT3 and CsatTFL1-3 may compete for binding to CsatFD2. To
525 investigate this, a luciferase complementation imaging (LCI) assay was conducted in
526 *Nicotiana benthamiana* leaves to evaluate the interaction strength between CsatFD2-
527 nLUC and cLUC-CsatTFL1-3 in the presence or absence of SK-CsatFT3.Strong
528 luciferase (LUC) activity was observed when CsatFD2-nLUC and cLUC-CsatTFL1-3
529 were coexpressed, indicating a robust interaction. However, coexpression with SK-
530 CsatFT3 significantly reduced LUC activity, suggesting that CsatFT3 interferes with
531 the interaction between CsatTFL1-3 and CsatFD2. Moreover, this suppression was
532 dose-dependent, with increasing amounts of CsatFT3 leading to a progressive
533 decrease in LUC signal (Figure 4E). Biological replicates supporting these
534 observations are presented in Supplementary figure 15 A and B. These results
535 strongly suggest that CsatFT3 competes with CsatTFL1-3 for interaction with
536 CsatFD2, which interferes with CsatTFL1-3's ability to interact with CsatFD2.
537
538 **CsatSVP2 Acts Upstream of FT3 in Temperature-Mediated Floral Repression**
539 To identify upstream genes potentially involved in temperature-dependent floral
540 induction in saffron, we screened transcriptome data representing the suppression of
541 floral induction under low temperatures (Jose-Santhi et al., 2023) and identified two

542 partial SVP-like MADS-box genes that were upregulated in non-flowering samples.
543 SVP-like genes are known to regulate flowering in a temperature-dependent manner
544 (Lee et al., 2007). Using long-read and other in-house transcriptome data, and based
545 on sequence similarity, we obtained full-length sequences of these two SVP-like
546 genes. We isolated and cloned them from saffron, naming them *CsatSVP1* and
547 *CsatSVP2*. Sequence analysis indicated that while these genes are highly similar, they
548 code for different amino acid sequences. Multiple sequence alignment revealed that
549 both CsatSVP1 and CsatSVP2 contain the conserved MADS-box domain, and
550 phylogenetic analysis grouped them with SVP-like genes from other geophytes, such
551 as Narcissus, Zingiber, and Lilium (Supplementary Figure 16 A and B).
552 To further characterize their role in flowering, we performed expression analysis of
553 *CsatSVP1* and *CsatSVP2* during vegetative and floral induction stages. Both genes
554 showed a significant reduction in expression during the floral induction stage (June);
555 however, the reduction in *CsatSVP2* was more pronounced and correlated closely with
556 floral induction and subsequent stages (Figure 5A). We then evaluated their
557 expression in corms stored under floral inductive (25°C) and non-inductive (8°C)
558 conditions. *CsatSVP2* transcript levels remained high at both temperatures,
559 suggesting it may contribute to the floral repression observed at low temperatures
560 (Figure 5C). In contrast, *CsatSVP1* expression decreased under both conditions,
561 showing no temperature-dependent pattern (Figure 5B). Additionally, *CsatSVP2*
562 expression was comparatively higher in floral tissues than *CsatSVP1*, further
563 supporting its potential regulatory role (Supplementary Figure 17).
564 Next, to functionally validate these genes, we ectopically expressed both *CsatSVP1*
565 and *CsatSVP2* in Arabidopsis under a constitutive promoter. Ectopic expression of
566 both genes resulted in delayed flowering, with a more pronounced delay in the
567 CsatSVP2-transformed lines compared to both the control and *CsatSVP1* lines (Figure
568 5D-I). Arabidopsis plants expressing *CsatSVP2* displayed various phenotypic changes
569 in flower bud and flower morphology, producing smaller, more compact flowers and
570 shorter siliques (Supplementary Figure 18). To investigate the role of *SVP* in
571 temperature-mediated floral suppression, we silenced *CsatSVP2* in saffron corms
572 using Virus-Induced Gene Silencing (VIGS). Csat*SVP2* was selected due to its
573 expression pattern and phenotype in Arabidopsis, which correlated with its expected
574 function. Since low temperatures during storage or dormancy are known to suppress
575 flowering, and CsatSVP2 may be involved in this process, we stored the *CsatSVP2*-

576 silenced corms at low temperatures, alongside a mock control (TRV2). Silencing of
577 SVP2 resulted in flowering in corms at low temperatures, whereas the TRV2-treated
578 corms stored at low temperatures did not flower (Figure 5J). In parallel, corms stored
579 at 25°C—an inductive condition—showed flowering in both control and SVP2-silenced
580 groups, confirming that *CsatSVP2* acts specifically in the floral suppression
581 mechanism under cold conditions (Figure 5K). Gene expression analysis further
582 revealed that *CsatSVP2* silencing prevented the typical low-temperature-mediated
583 suppression of *CsatFT3* expression, thereby facilitating flowering (Figure 5P and Q).
584 These findings suggest that CsatSVP2 and CsatFT3 act within the same regulatory
585 pathway, mediating temperature-responsive floral induction in saffron.
586
587 **SVP2 Directly Binds to the CsatFT3 Promoter and Represses Its Expression**
588 Our previous results indicated that CsatSVP2 and CsatFT3 function in the same
589 temperature-sensitive regulatory pathway: low temperature maintains or upregulates
590 CsatSVP2 expression, which in turn suppresses *CsatFT3*, thereby repressing floral
591 induction. Notably, *CsatFT3* transcript levels were restored in *CsatSVP2*-silenced
592 corms, suggesting that CsatSVP2 functions upstream of *CsatFT3*. To further explore
593 the mechanism of this regulation, we analyzed the CsatFT3 promoter sequence to
594 identify potential binding motifs for MADS-box transcription factors. In silico analysis
595 of the 1.2 kb FT3 promoter, previously shown to drive temperature-responsive
596 expression, revealed a conserved CArG-box motif (CCATTTAAGG) located
597 approximately 827 bp upstream of the ATG start codon that is established for binding
598 of MADS boxes genes including SVP orthologs (Figure 6A). To experimentally test
599 further whether CsatSVP2 directly binds to the *CsatFT3* promoter, we performed a
600 yeast one-hybrid (Y1H) assay. The Y1H assay confirmed that CsatSVP2 specifically
601 binds to the *CsatFT3* promoter, supporting the hypothesis of direct regulation (Figure
602 6B). To further validate the functional specificity of this interaction, we employed a
603 luciferase reporter assay using *Nicotiana benthamiana* transient expression (Figure
604 6C) and conducted a luciferase reporter assay using three different FT3 promoter
605 fragments: (1) the full-length promoter (~1.2kb), (2) a truncated version containing the
606 conserved CArG motif (T1), and (3) a truncated version lacking the motif (T2) (Figure
607 6D). Co-expression of CsatSVP2 with these constructs in *Nicotiana benthamiana*
608 revealed that luciferase activity was significantly reduced in both the full-length and T1
609 constructs (Figure6 D and F). In contrast, no repression was observed with the T2

construct, confirming that SVP2 specifically suppresses FT3 expression through direct binding to the CArG motif (Figure 6F). Together, these results establish a mechanistic model in which CsatSVP2 acts as a temperature-responsive floral repressor that directly binds to the FT3 promoter via a conserved CArG motif, thereby repressing FT3 expression and floral induction under low-temperature conditions.

Discussion

Saffron is a high-value crop cultivated in limited regions due to its strict temperature requirements, which distinctly regulate its vegetative and reproductive growth. High temperatures induce flowering, while subsequent cooling triggers flower formation. In contrast, low temperatures suppress floral induction and support vegetative growth, enabling overwintering and daughter corm development (Molina et al., 2005a). This temperature sensitivity restricts saffron cultivation to specific climates. Although environmental control of flowering has enabled cultivation in soilless and controlled settings, the molecular mechanisms underlying temperature-regulated flowering remain poorly understood. As a sterile crop, saffron cannot be improved through conventional breeding, making biotechnological interventions essential. However, limited genomic and genetic resources, challenges in genetic transformation, and a scarcity of molecular studies have hindered progress in functional genomics—creating a critical knowledge gap that must be addressed.

In this study, we have identified a temperature-sensitive transcriptional network that regulates flowering in saffron, uncovering both conserved and saffron-specific components involved in floral induction (Figure 7). Our data establish a regulatory module involving CsatFT3, CsatFD2, CsatTFL1-3/CEN1, and CsatSVP2 as key components in mediating floral transition in response to temperature cues. Although the core elements of the Florigen Activation Complex (FAC)—FT, FD, and TFL1—are conserved across angiosperms, their expression patterns, protein interactions, and functional dynamics in saffron suggest neofunctionalization in line with its geophytic lifecycle. For instance, Notably, CsatFT3 and CsatFD2 are upregulated at higher temperatures and co-expressed in the floral meristem, promoting flowering. In contrast, other FT and FD homologs show no such expression correlation (Figure 2; (Kalia et al., 2022), indicating their limited or no involvement in floral induction. Similarly, CsatTFL1-3 functions as a floral repressor by competitively binding to CsatFD2, whereas the other two TFL1 homologs neither interact with CsatFD2 nor

644 delay flowering in Arabidopsis, suggesting a lack of functional redundancy and
645 functional specificity. Functional validation in both Arabidopsis and saffron confirms
646 that floral induction is governed by the dynamic interplay between CsatFT3, CsatFD2,
647 and CsatTFL1-3.Given the roles of gene duplication, neofunctionalization, and
648 lineage-specific gene expansion in driving the specialization of reproductive and
649 vegetative pathways in geophytes (Khosa et al., 2021), our identification of distinct
650 regulatory factors and their molecular interactors from multigene families in saffron
651 represents a significant advance.
652 A distinguishing feature of floral induction observed in saffron is the spatial restriction
653 of flowering-related gene expression predominantly to the meristem. All the genes
654 identified in this study were specifically expressed in the apical (flowering) meristem.
655 During floral induction, saffron corms are either underground or stored in the dark and
656 remain leafless, indicating that the molecular signals initiating flowering are localized
657 within the apical buds. Such meristem-localized control may reflect an adaptation to
658 the geophytic habit of saffron, which undergoes floral induction in the absence of
659 foliage, similar to what has been observed in other geophytes such as tulips
660 (Leeggangers et al., 2017b). This localization supports the hypothesis that
661 temperature cues are sensed and interpreted locally within the corm, rather than
662 systemically via leaves, as observed in many other species, including some geophytes
663 (Lee et al., 2013b; Navarro et al., 2011; Wigge, 2011; Wu et al., 2022; Yan et al.,
664 2021).
665 Temperature plays a pivotal role in regulating flowering time across plant species,
666 often through conserved thermosensory pathways. In Arabidopsis, warmer
667 temperatures promote flowering via *FT* activation (Balasubramanian et al., 2006).
668 while in crops like strawberry and onion, cold exposure induces flowering by triggering
669 FT-like genes (Heide, 1977; Lee et al., 2013b). Interestingly, the effect of temperature
670 on flowering is not always straightforward. Temperatures above 25°C seem to have
671 both inductive and repressive effects on flowering, depending on the species and
672 environmental conditions (Nakano et al., 2013; Noy-Porat et al., 2013; Oda et al.,
673 2012). This temperature sensitivity is closely linked to the regulation of FT, a key gene
674 that integrates various environmental signals and controls the timing of flowering. In
675 *Narcissus tazetta* (daffodils), floral induction is triggered by high ambient temperatures
676 (25°C) through the activation of *NtFT*, while in tulips, *TgTFL1* downregulation and
677 *TgFT2* upregulation contribute to temperature-induced floral induction (Leeggangers

678 et al., 2017a; Noy-Porat et al., 2013). In contrast, in species like onion and lily, which
679 flower in spring, vernalization (low-temperature treatment) is required to activate the
680 expression of *AcFT2* and *LiFT*, respectively (Lee et al., 2013b). In our study, we also
681 found that *CsatFT3*, a key flowering-time gene in saffron, is temperature-regulated,
682 with its expression being induced by high ambient temperatures and suppressed by
683 low temperatures (Figure 1B). Similarly, *CsatFD2*, a partner of *CsatFT3* in the
684 flowering regulatory network, follows a similar expression pattern, suggesting their
685 involvement in the temperature-mediated floral induction pathway in saffron.
686 Interestingly, we observed that *CsatTFL1-3*, a gene that maintains the vegetative state
687 and prevents early flowering, exhibits a reciprocal expression pattern. In Arabidopsis
688 low and ambient temperature regulation of flowering involves the gene *TFL1* (Strasser
689 et al., 2009). Higher expression of *CsatTFL1-3* is observed during the vegetative
690 phase, which coincides with the low winter temperatures during saffron's growth cycle
691 (Figure 3A). This expression pattern is crucial for maintaining the vegetative phase
692 and delaying flowering, as confirmed by the hyper-vegetative shoot phenotype in
693 *TFL1*-3 overexpressing Arabidopsis plants (Figure 3) similar to what was observed
694 when Arabidopsis *TFL1* is overexpressed (Lee et al., 2019). In contrast, as
695 temperatures rise in the summer, the expression of CsatFT3 increases (Figure 1A),
696 likely triggering the activation of floral pathway genes and the transition to reproductive
697 development. Overall, a balance between CsatFT3, CsatTFL1-3, and their interaction
698 with CsatFD2 governs floral induction in a temperature-dependent manner. This
699 delicate interplay between temperature and gene expression is vital for ensuring
700 proper timing of flowering in saffron, aligning the plant's reproductive phase with
701 favourable environmental conditions.
702 We also identify CsatSVP2, a MADS-box transcription factor, as a critical floral
703 repressor acting upstream of FT–FD–TFL core module. MADS-box genes are key
704 regulators of flowering time, with SVP-like genes playing central roles in ambient
705 temperature-mediated floral control (Jin and Ahn, 2021). CsatSVP2 directly binds a
706 conserved CArG-box in the CsatFT3 promoter, repressing its expression under low
707 temperatures. Silencing of SVP2 alleviated low-temperature-induced flowering
708 suppression and restored *CsatFT3* expression, thereby establishing a direct
709 mechanistic link between ambient temperature perception and floral induction (Figure
710 5). In *Arabidopsis thaliana*, a comparable regulatory pathway has been described,
711 where SVP negatively regulates FT expression by directly binding to a CArG motif in

its promoter (Lee et al., 2007). Additionally, SVP levels are known to increase under low temperatures and are degraded at higher temperatures, facilitating early flowering as SVP abundance declines (Blázquez et al., 2002; Lee et al., 2013a; Sureshkumar et al., 2016). Interestingly, individual members of the SVP gene family have been shown to play distinct roles in processes such as bud dormancy, flowering initiation, and floral development reflecting adaptations of developmental timing to local environmental conditions and seasonal temperature fluctuations. In tulips, gene expression analyses have similarly identified *TgMADS15*/*16* and *TgMADS9* as low-temperature-responsive SVP-like genes involved in floral induction (Lu et al., 2023), reinforcing the conserved role of this gene family in temperature-mediated flowering regulation across geophytic species. SVP homologs in Lilium and *Narcissus tazetta* have also been reported as flowering repressors, though their temperature responsiveness remains unexplored (Li et al., 2015; Wu et al., 2024). Notably, ectopic expression of *CsatSVP2* in Arabidopsis caused floral morphology defects, reminiscent of phenotypes observed with Lilium SVP expression (Wu et al., 2024), suggesting that these homologs may also contribute to flower development in addition to regulating flowering time.

Conclusion

Collectively, our findings establish a detailed molecular framework for temperature-regulated flowering in saffron, centered on the dynamic balance between floral activators (CsatFT3, CsatFD2) and repressors (CsatTFL1-3, CsatSVP2). The spatiotemporal expression patterns and protein interactions among these components provide key insights into how flowering is precisely modulated in response to environmental temperature fluctuations. By uncovering saffron-specific adaptations within otherwise conserved gene networks, this study advances our understanding of floral regulation in geophytes and sterile crops. Importantly, these results lay a foundation for the development of genetic and biotechnological strategies to improve saffron yield, synchronize flowering, and enhance resilience to climate variability. Our work highlights a saffron-specific model of thermoresponsive flowering that builds upon conserved floral regulatory pathways, yet exhibits functional divergence shaped by the geophytic lifecycle. Beyond saffron, these findings offer a valuable framework for translational research in other temperature-sensitive geophytes such as tulip, Narcissus, Hyacinthus, and Iris, where molecular insights remain scarce (Khodorova

746 and Boitel-Conti, 2013). By identifying novel regulatory targets, this study opens new
747 avenues for improving flowering and productivity in saffron and related high-value
748 geophytic species.
749
750 **Acknowledgments**
751 We gratefully acknowledge the financial support from the Council of Scientific and
752 Industrial Research (CSIR) under the Genome Editing Mission for Crop Improvement
753 (MMP25301), the intramural CSIR grant to IHBT (MLP201), the SERB-Start-up
754 Research Grant (SRG/GAP0288), and the Department of Biotechnology
755 (DBT/GAP0307) to Rajesh Kumar Singh. Senior Research Fellowships provided to
756 Diksha Kalia (UGC), Joel Jose-Santhi (CSIR), and Firdous Rasool Sheikh (CSIR) are
757 also gratefully acknowledged. We sincerely thank Dr. Rishikesh Bhalerao, Umeå Plant
758 Science Centre, Swedish University of Agricultural Sciences, Sweden, for his careful
759 reading of the manuscript and for providing constructive feedback, which significantly
760 improved the clarity and quality of the work. Our sincere thanks go to Dr. Rimpy Diman,
761 Technical Officer at CSIR-IHBT, for her valuable assistance with confocal microscopy.
762 This manuscript represents the CSIR-IHBT communication number "5819".
763
764 **Author contribution statement**
765 R.K.S. conceptualized the research idea and designed the work plan. D.K., J.J.S., and
766 F.R.S. conducted the experiments and collected the data. D.K., J.J.S., and R.K.S.
767 analyzed the data and contributed to writing the manuscript. All authors read and
768 approved the final version of the manuscript.
769
770 **Conflicts of Interest**
771 The authors declare no conflicts of interest.
772
773 **Figure Legends**
774 **Figure 1. *CsatFT3* is involved in temperature mediated floral induction in saffron.**
775 **(A)** CsatFT3 transcript levels in apical buds across developmental stages show
776 specific expression during the reproductive phase. **(B)** Relative expression of CsatFT3
777 in apical buds of saffron corms stored at ambient (25°C) and low (8°C) temperatures.
778 Data are means ± SEM from 3 biological replications, where n=10 for each replicate.
779 **(C)** Histochemical GUS assay of the *CsatFT3* promoter (proCsatFT3) in transgenic

780 Arabidopsis in long-day conditions (LD) during various developmental stages. 1.2kb
781 sequence upstream of the CsatFT3 translation start sites (proCsatFT3) was fused with
782 uidA (GUS) reporter gene. Different developmental stages include Arabidopsis plants
783 after 7 Days After Germination (DAG), 14DAG, 21DAG, and 30DAG. FT3 expression
784 is confined to meristem and inflorescence **(D)** Temperature sensitive GUS activity at
785 3 different temperatures. The experiment was repeated three times independently with
786 similar results. **(E-G)** Ectopic expression of CsatFT3 in Arabidopsis resulted in early
787 flowering phenotype. Statistical significance was analyzed by Student's t-test (*P <
788 0.05). **(H-J)** Functional complementation of the ft-10 mutant with CsatFT3 restores
789 flowering. Representative line expressing number of rosette leaves and number of
790 days to flower. Total leaf number was calculated by combining total rosette leaves.
791 Data represent a minimum of 10 plants scored for each line. Statistical significance
792 was analyzed by Student's t-test (*P < 0.05). **(K)** Representative flowering vs. non-
793 flowering phenotypes in control and CsatFT3-silenced saffron corms. The scale bar
794 represents 2 cm. **(L)** qRT-PCR validation of CsatFT3 transcript knockdown in saffron
795 corm apices following VIGS (n=3 technical replicates, 10 independent corms). Error
796 bars are shown as Standard Error of Mean (SEM) of three technical repeats. **(M)**
797 Percentage of flowering in VIGS-silenced vs. TRV2 control corms. The data presented
798 includes the mean percentage of flowering, with error bars representing the Standard
799 Error of Mean (SEM) of three technical repeats (n=3) and for each replicate, 10 corms
800 were used. All data in this figure are shown as mean ± SEM. Statistical Significance
801 for Data in panel A, I, & J are analyzed using one-way ANOVA followed by Tukey's
802 Honest Significant Difference (HSD) test for multiple comparisons. Different letters
803 indicate statistically significant differences between groups at p < 0.05, according to
804 Compact Letter Display (CLD). Data in panels B are analyzed using two-way ANOVA
805 to assess the effects of temperature, month, and their interaction, followed by Sidak's
806 multiple comparisons test. Asterisks indicate significant differences between 8°C and
807 25°C within each month (**** p < 0.0001), F, **G**, **L**, and **M** are analyzed using the
808 student's t-test (*: p<0.05; **: p<0.01).
809
810 **Figure 2: Functional characterization of FD-like genes in saffron (A)** Expression
811 profiles of CsatFD1, CsatFD2, and CsatFD3 during vegetative and floral induction
812 stages in the apical bud by RT-qPCR. Data are means ± SE of 3 independent
813 replicates. **(B)** Expression patterns of CsatFD1, CsatFD2, and CsatFD3 in the Main

814 bud (MB), axillary bud (AB), and corm tissue (CT) during the floral induction stage.
815 Values are means ± SE of 3 independent replicates. **(C)** Tissue specific expression of
816 FDs in different parts of saffron plant. **(D)** Expression analyses of *CsatFD* genes in
817 apical buds of corms stored at 25◦ C and 8 during months of May and June (**E)**
818 Phenotypic comparison of early flowering in CsatFD2-expressing Arabidopsis
819 compared to control. **(F-K)** Measurements of days to flowering and rosette leaf number
820 in CsatFD1, CsatFD2, and CsatFD3 expressing Arabidopsis plants. Values are means
821 ± SE (n = 10). Asterisks indicate a significant difference between the transgenic
822 Arabidopsis lines and wild-type plants (Col-0; Student's t-test, P < 0.05). **(L)**
823 Phenotypes of CsatFD2-TRV2 silenced lines and TRV2 lines. The scale bar
824 represents 2 cm. **(M)** qRT-PCR validation of CsatFD2 knockdown in saffron corm
825 apices after VIGS (n=3). Error bars are shown as SD of three technical repeats **(N)**
826 Flowering percentage in TRV2 control and CsatFD2 VIGS-silenced saffron corms. The
827 data presented includes the mean percentage of flowering, with error bars
828 representing the standard error of mean (SEM) of three technical repeats (n=3) and
829 for each replicate, 10 corms were used. All data in this figure are shown as mean ±
830 SEM. Statistical Significance for data in panel **A** & **B** are analyzed using two-way
831 ANOVA followed by Tukey's Honest Significant Difference (HSD) test for multiple
832 comparisons. Different letters indicate statistically significant differences between
833 groups at p < 0.05, according to Compact Letter Display (CLD). Data in panel **D** are
834 analyzed using two-way ANOVA to assess the effects of temperature, month, and their
835 interaction, followed by Sidak's multiple comparisons test. Asterisks indicate
836 significant differences between 8°C and 25°C within each month (**** p < 0.0001), ,
837 **F**,**G**,**H**,**I**,**J**,**K**,**M** and **N** are analyzed using the Student's t-test (*: p<0.05; **: p<0.01).
838
839 **Figure 3: CsatTFL1-3 is negative regulator of floral induction in saffron (A)**
840 Relative expression of CsatTFL1-3 during vegetative and reproductive phase in the
841 apical bud by RT-qPCR. Data are means ± SE of 3 independent replicates. **(B)**
842 Expression analyses of CsatTFL1-3 gene in apical buds of corms stored at 25°C and
843 8 °C during floral induction time **(C)** Corm tissue specific expression of TFL1-3 during
844 floral induction. **(D)** Tissue Specific Expression of CsatTFL1-3. **(E)**Phenotypic analysis
845 of Arabidopsis Col-0 plants ectopically expressing TFL1-3/CEN1, Hyper vegetive
846 phase phenotype observed in CsatTFL1-3 transgenic lines of Arabidopsis. **(F and G)**
847 Rosette leaves number and number of days to flower of 35S::TFL1-3 transgenic and

848 control plants respectively. Values are means ± SEM (n = 10). Asterisks indicate a
849 significant difference between the transgenic Arabidopsis lines and wild-type plants
850 (Col-0; Student's t-test, P < 0.05). **(H)** Virus-Induced Gene Silencing (VIGS) of TFL1-
851 3/CEN1 in low-flower-competent saffron corms. The scale bar represents 2 cm. **(I)** The
852 expression of *CsatTFL1-3* in *CsatTFL1-3*-TRV2 silenced lines and TRV2 lines (n=3).
853 **(J)** Comparison of flowering percentages in VIGS-silenced versus control saffron
854 corms. The data presented includes the mean percentage of flowering of three
855 technical repeats (n=3) and for each replicate, 10 corms were used. All data in this
856 figure are shown as mean ± SEM. Statistical Significance for Data in panel **A**,**C** & **D**
857 are analyzed using one-way ANOVA followed by Tukey's Honest Significant
858 Difference (HSD) test for multiple comparisons. Different letters indicate statistically
859 significant differences between groups at p < 0.05, according to Compact Letter
860 Display (CLD). Data in panel B are analyzed using two-way ANOVA to assess the
861 effects of temperature, month, and their interaction, followed by Sidak's multiple
862 comparisons test. Asterisks indicate significant differences between 8°C and 25°C
863 within each month (**** p < 0.0001), , F,G,I, & J are analyzed using the Student's t-
864 test (*: p<0.05; **: p<0.01).
865
866 **Figure 4. Interaction analysis of CsatFT3, CsatTFL1-3, and CsatFD2.**
867 **(A, B)** Yeast two-hybrid (Y2H) assays showing physical interactions between
868 CsatFT3/CsatTFL1-3 and CsatFD2. The coding sequences of *CsatFT3* and
869 *CsatTFL1-3* were fused to the activation domain in the pGADT7 vector, and *CsatFD2*
870 was fused to the DNA-binding domain in the pGBKT7 vector. Yeast transformants
871 were grown on double dropout (DDO) medium lacking tryptophan and leucine
872 (selection for transformation) and quadruple dropout (QDO) medium lacking
873 tryptophan, leucine, histidine, and adenine (selection for interaction). pGBKT7-53 and
874 pGADT7-T were used as positive control; pGBKT7-lam and pGADT7-T interactions
875 served as the negative control. **(C-D)** Bimolecular fluorescence complementation
876 (BiFC) assay showing nuclear localization of the interactions between CsatFT3 or
877 CsatTFL1-3 with CsatFD2 in *Nicotiana benthamiana* leaf epidermal cells. CsatFD2
878 was fused to the C-terminal half of YFP (cYFP), and CsatFT3 or CsatTFL1-3 were
879 fused to the N-terminal half of YFP (nYFP). YFP signal indicates interaction. Bars =
880 20 μm. **(E)** Competitive luciferase complementation assay demonstrating the
881 competition between CsatFT3 and CsatTFL1-3 for binding to CsatFD2 in *N.*

882 *benthamiana* leaves. CsatTFL1 was fused to the N-terminal half of luciferase (nLUC),
883 and CsatFD2 to the C-terminal half (cLUC). Increasing amounts of CsatFT3 (non-
884 tagged, driven by 35S promoter, in SK vector) were co-infiltrated at different ratios.
885 Images represents three independent replications. **(F)** Relative luminescence
886 intensities indicate competition for FD2 binding with TFL1-3 and FT3. Data
887 represented is mean of three replicates. Statistical Significance are analyzed using
888 one-way ANOVA followed by Tukey's Honest Significant Difference (HSD) test for
889 multiple comparisons. Different letters indicate statistically significant differences
890 between groups at $p < 0.05$, according to Compact Letter Display (CLD).
891
892 **Figure 5: Functional characterization of CsatSVP1 and CsatSVP2 in**
893 **temperature-dependent floral regulation (A)** Expression profiling of CsatSVP1 and
894 CsatSVP2 in apical bud during different vegetative and flowering stages. Data are
895 means ± SE from 3 replications. **(B and C)** Expression of SVP1 and SVP2 genes in
896 corms stored at inductive (25°C) and non-inductive (8°C) temperatures respectively.
897 **(D)** Flowering phenotypes of Arabidopsis lines ectopically expressing CsatSVP1. **(E**
898 **and F)** Rosette leaves number and number of days to flower of CsatSVP1 transgenic
899 and control plants respectively **(G)** Phenotypic changes of the floral organs in
900 35S::CsatSVP2 transgenic Arabidopsis plants. **(H-I)** Rosette leaves number and
901 number of days to flower of CsatSVP2 transgenic and control plants respectively. The
902 total leaf number was calculated by combining total rosette leaves. **(J-K)** Silencing of
903 CsatSVP2 by VIGS rescues flowering under low-temperature conditions in saffron.
904 The scale bar represents 2 cm. **(L-M)** qRT-PCR validation of CsatSVP2 knockdown in
905 saffron corm apices after VIGS stored at different temperatures (n=3). Error bars are
906 shown as SD of three technical repeats. **(N-O)** Flowering percentage in TRV2 control
907 and CsatSVP2 VIGS-silenced saffron corms stored at low (8°C) and ambient (23°C)
908 temperatures. The data presented includes the mean percentage of flowering, with
909 error bars representing the standard deviation (SD) of three technical repeats (n=3)
910 and for each replicate, 10 corms were used. **(P-Q)** Relative expression of CsatFT3 in
911 SVP2-silenced versus control corms under different temperature regimes. All data in
912 this figure are shown as mean ± SEM. Statistical Significance for data in panel A are
913 analyzed using two-way ANOVA followed by Tukey's Honest Significant Difference
914 (HSD) test for multiple comparisons. Different letters indicate statistically significant
915 differences between groups at $p < 0.05$, according to Compact Letter Display (CLD).

916 Data in panel B & C are analyzed using two-way ANOVA to assess the effects of
917 temperature, month, and their interaction, followed by Sidak's multiple comparisons
918 test. Asterisks indicate significant differences between 8°C and 25°C within each
919 month (**** $p < 0.0001$), E, F, H, I, L, M, N, O, P & Q are analyzed using the student's
920 t-test (*: $p<0.05$; **: $p<0.01$).
921
922 **Figure 6. CsatSVP2 directly binds to the FT3 promoter via the CArG motif and**
923 **represses its transcription (A)** Schematic diagram of the 1.2 kb CsatFT3 promoter
924 showing the location of a conserved CArG-box motif (CCATTTAAGG) approximately
925 827 bp upstream of the ATG start codon. **(B)** Yeast one-hybrid assay showing
926 interaction between CsatSVP2 and the FT3 promoter region containing the CArG
927 motif. Growth on selective media confirms binding specificity. **(C)** Schematic diagram
928 of the effectors and reporters used in dual-luciferase reporter. **(D)** Schematic of the
929 dual-luciferase constructs used for transient expression in *Nicotiana benthamiana*: FL
930 (Full length promoter) T1 (with CArG motif) and T2 (without). **(E)** Relative luciferase
931 activity in leaves co-expressing CsatSVP2 with the full promoter and T1 fragment
932 construct of *CsatFT3* gene. **(F)** Relative luciferase activity in leaves co-expressing
933 CsatSVP2 and CsatFT3 full promoter and with T2 fragment constructs. Significant
934 repression is observed only in the T1 construct, indicating that CsatSVP2 represses
935 *CsarFT3* transcription through the CArG motif. **(G and H)** Quantification of luciferase
936 activity. Bars represent mean ± SEM (n = 3). All data in figure are shown as mean ±
937 SEM. Statistical Significance for Data in panel **F** & **H** are are analyzed using one-way
938 ANOVA followed by Tukey's Honest Significant Difference (HSD) test for multiple
939 comparisons. Different letters indicate statistically significant differences between
940 groups at $p < 0.05$, according to Compact Letter Display (CLD)
941
942 **Figure 7. Proposed model of temperature-mediated flowering regulation in**
943 **saffron.** This schematic model illustrates the temperature-regulated floral induction
944 pathway in saffron, emphasizing the key roles of CsatFT3, CsatFD2, TFL1-3/CEN1,
945 and CsatSVP2 in transitioning from vegetative to reproductive growth. At low
946 temperatures (e.g., below 10°C), *CsatFT3* expression remains low, preventing the
947 formation of the Floral Activator Complex (FAC). TFL1-3/CEN1 binds to CsatFD2,
948 maintaining the shoot apical meristem in a vegetative state and inhibiting flowering.
949 *CsatFD2* expression is minimal, suppressing floral induction. At low temperatures,

950 *CsatSVP2* is upregulated and directly binds to the FT3 promoter at a conserved CArG
951 motif, repressing its expression and preventing FAC formation. As temperatures rise
952 above the threshold (e.g., 25°C), *CsatFT3* expression increases, leading to the
953 formation of the FAC by binding to CsatFD2. This complex activates the expression of
954 floral meristem identity genes and promotes floral development. At the same time,
955 *TFL1-3/CEN1* expression decreases, allowing the activation of CsatFD2 and the
956 initiation of flowering.
957
958
959
960
961
962
963
964
965
966
967
968
969
970
971
972
973
974
975
976
977
978
979
980
981
982
983

984 **Figure 1**

985

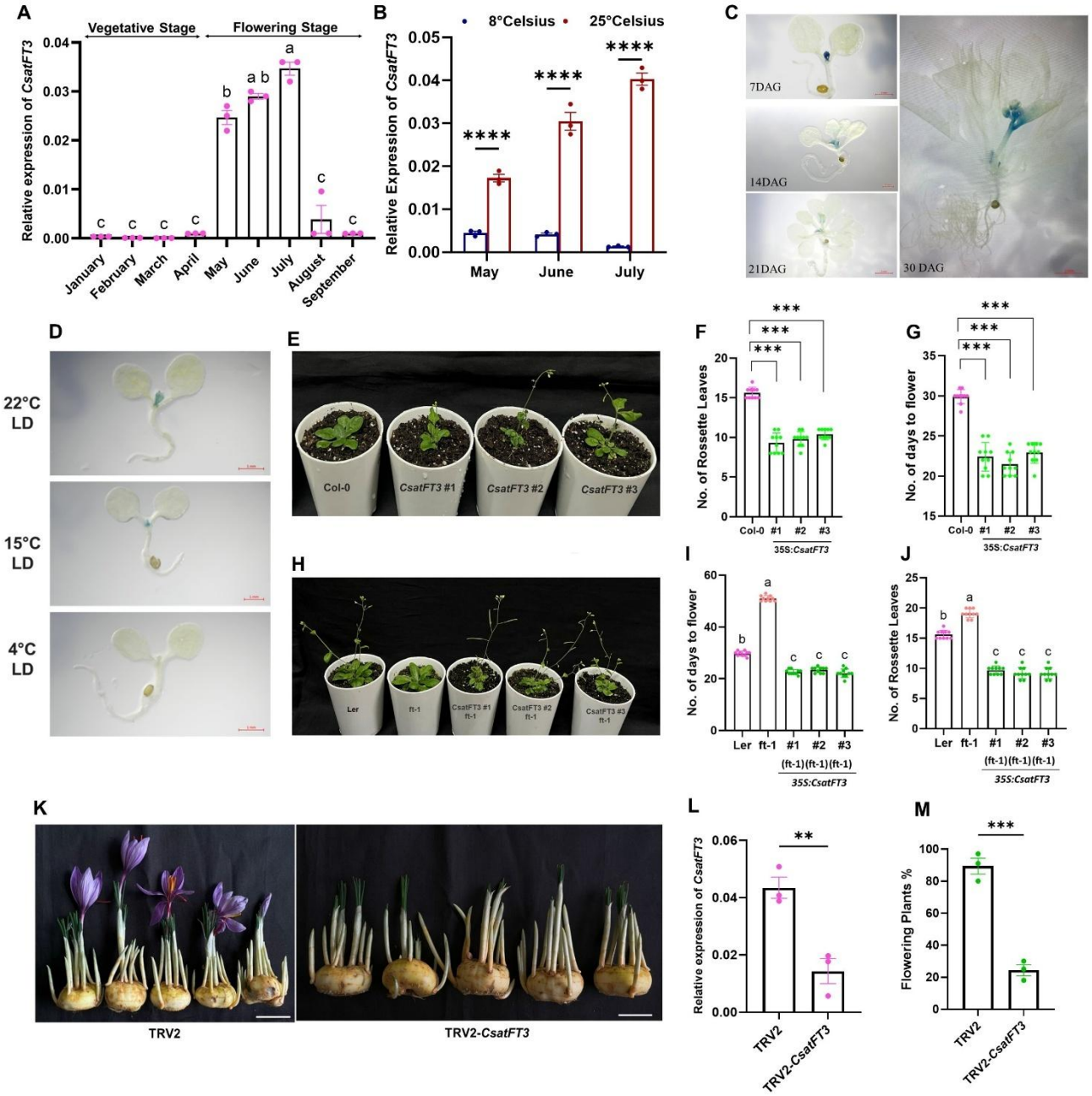

986

987

988

989

990

991

992

993

994 **Figure 2**

995

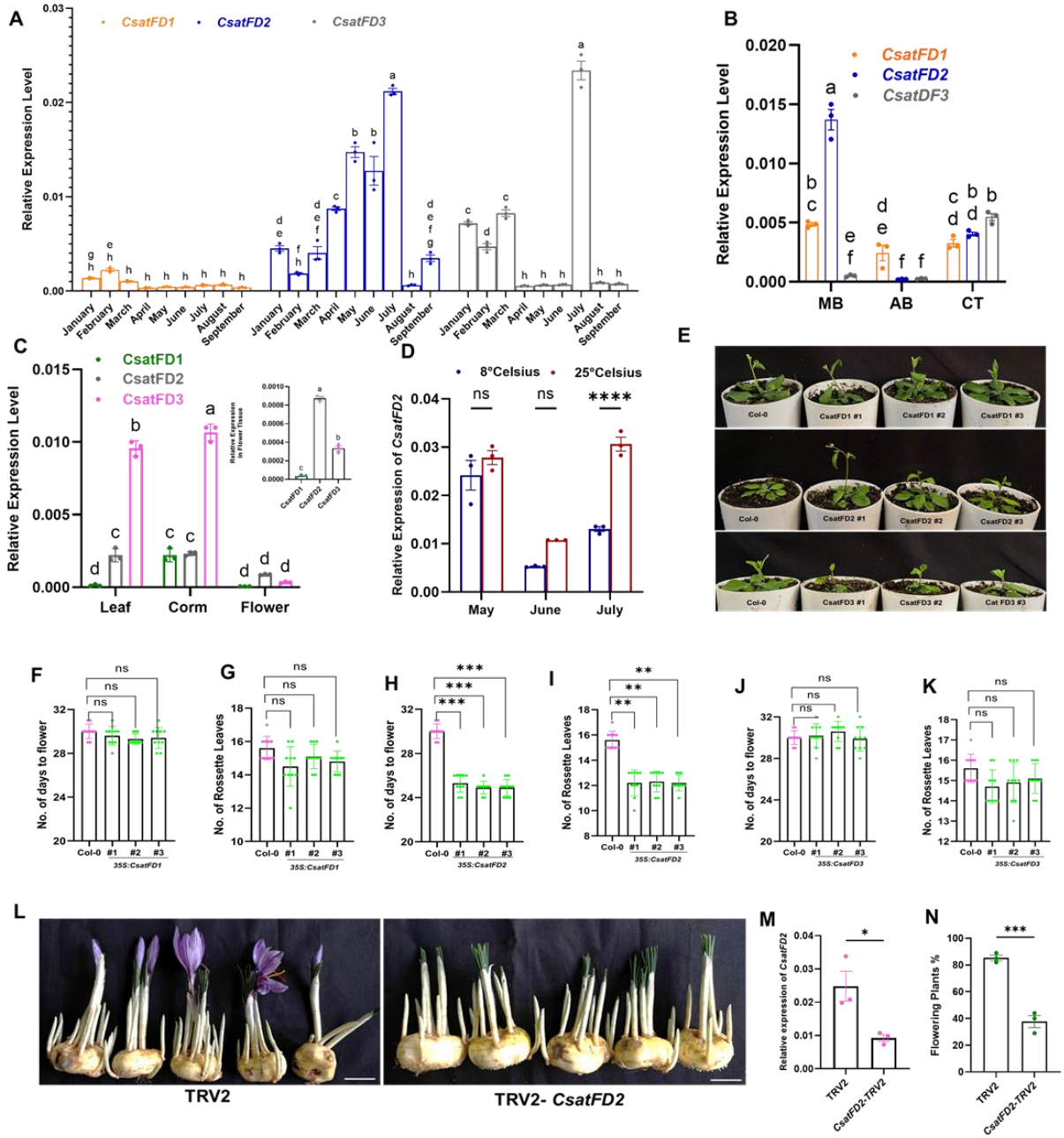

996

997

998

999

1000

1001

1002

1003

1004 **Figure 3**

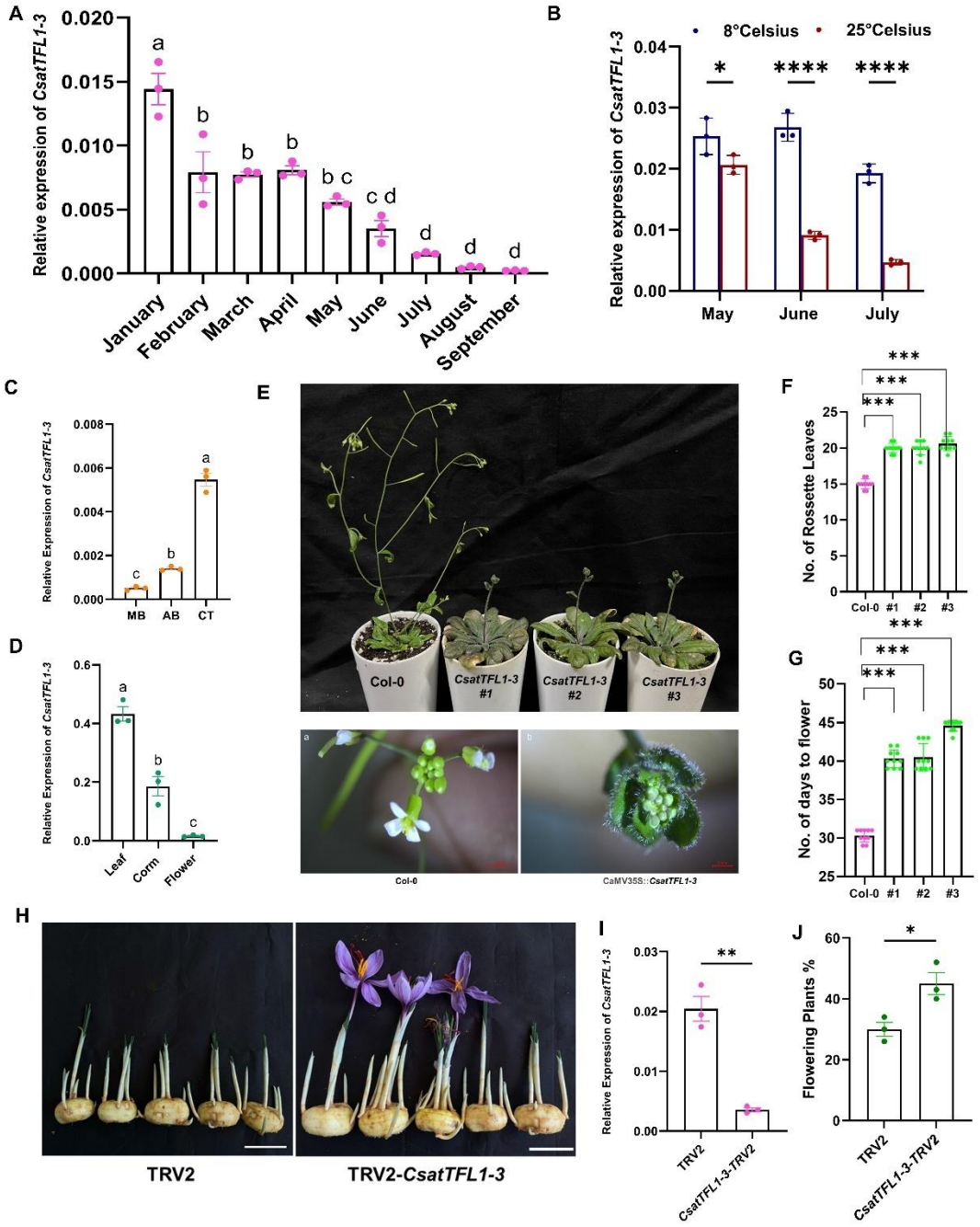

1005

1006

1007

1008

1009

1010

1011

1012

1013 **Figure 4**

1014

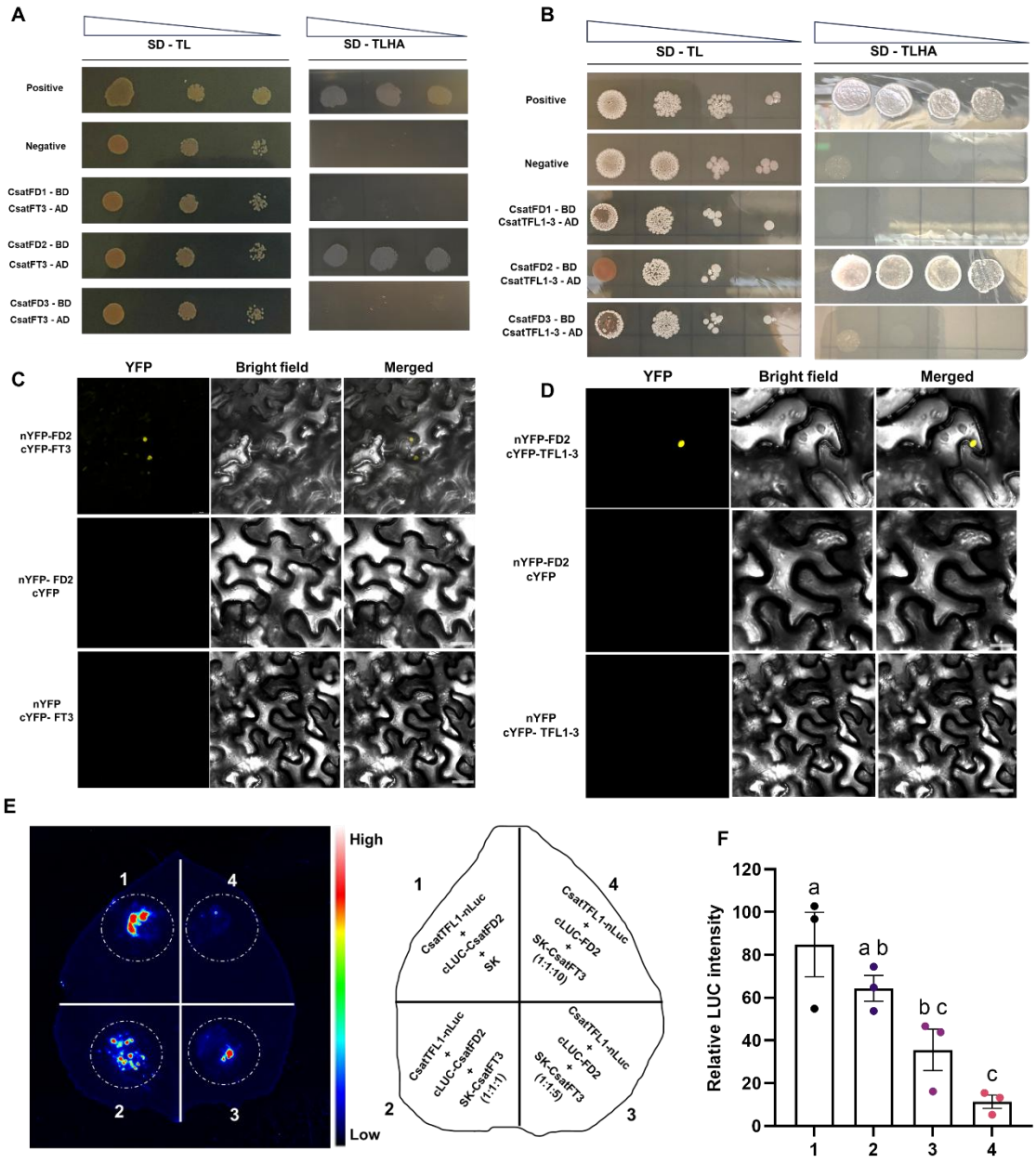

1015

1016

1017

1018

1019

1020

1021

1022

1023

1024 **Figure 5**

1025

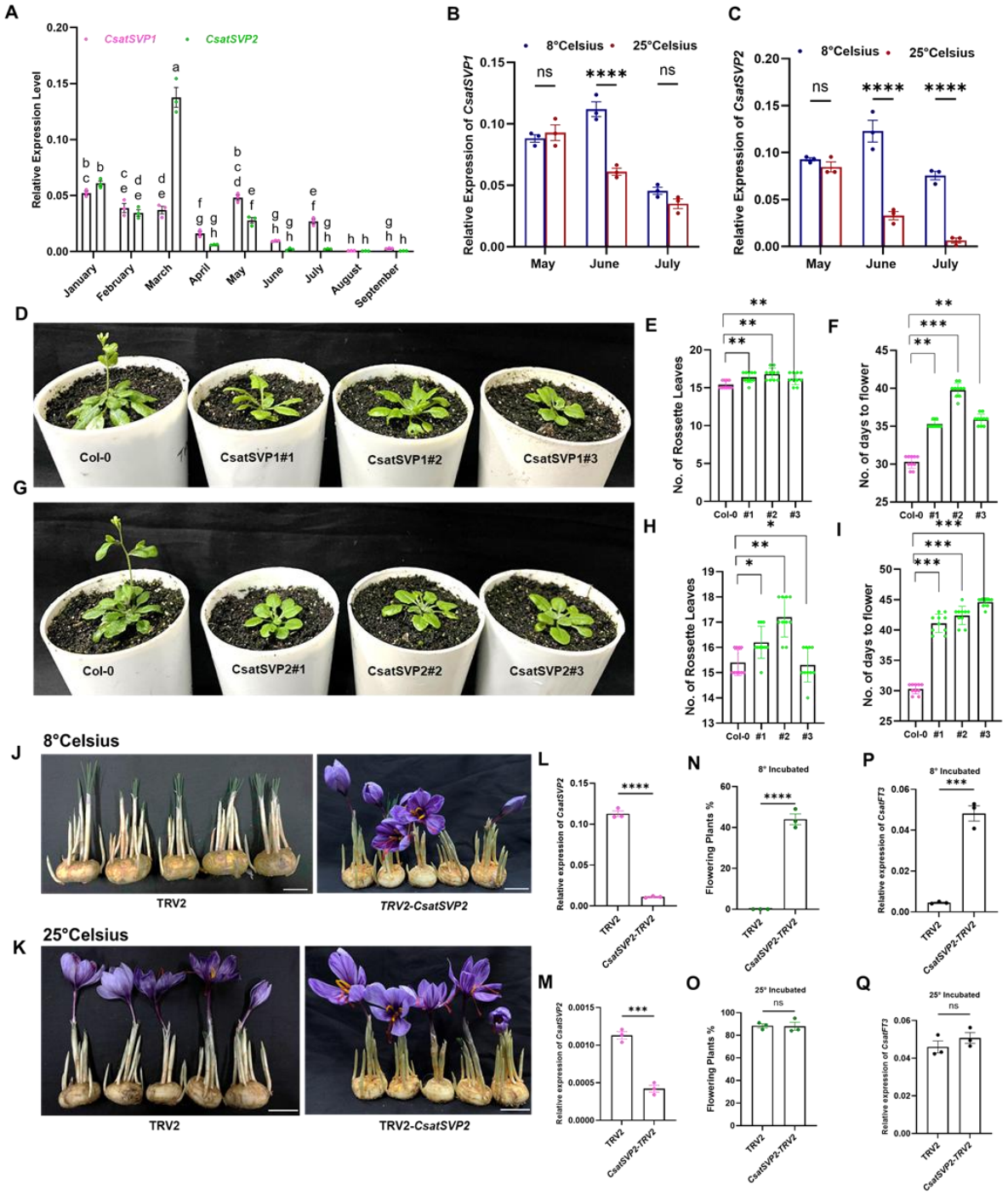

1026

1027

1028

1029

1030

1031

1032

1033 **Figure 6**

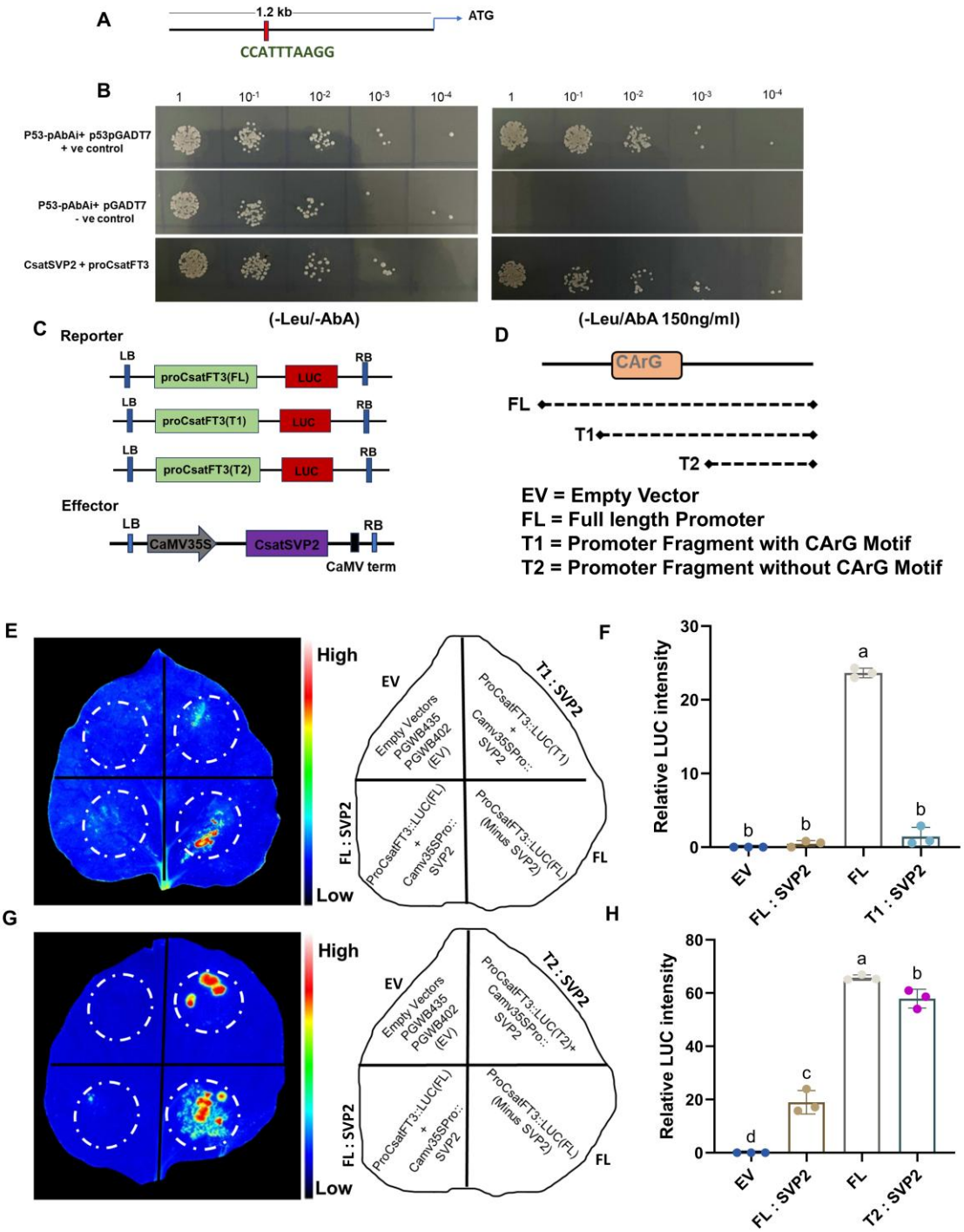

1034

1035

1036

1037

1038

1039

1040

1041 **Figure 7**

1042

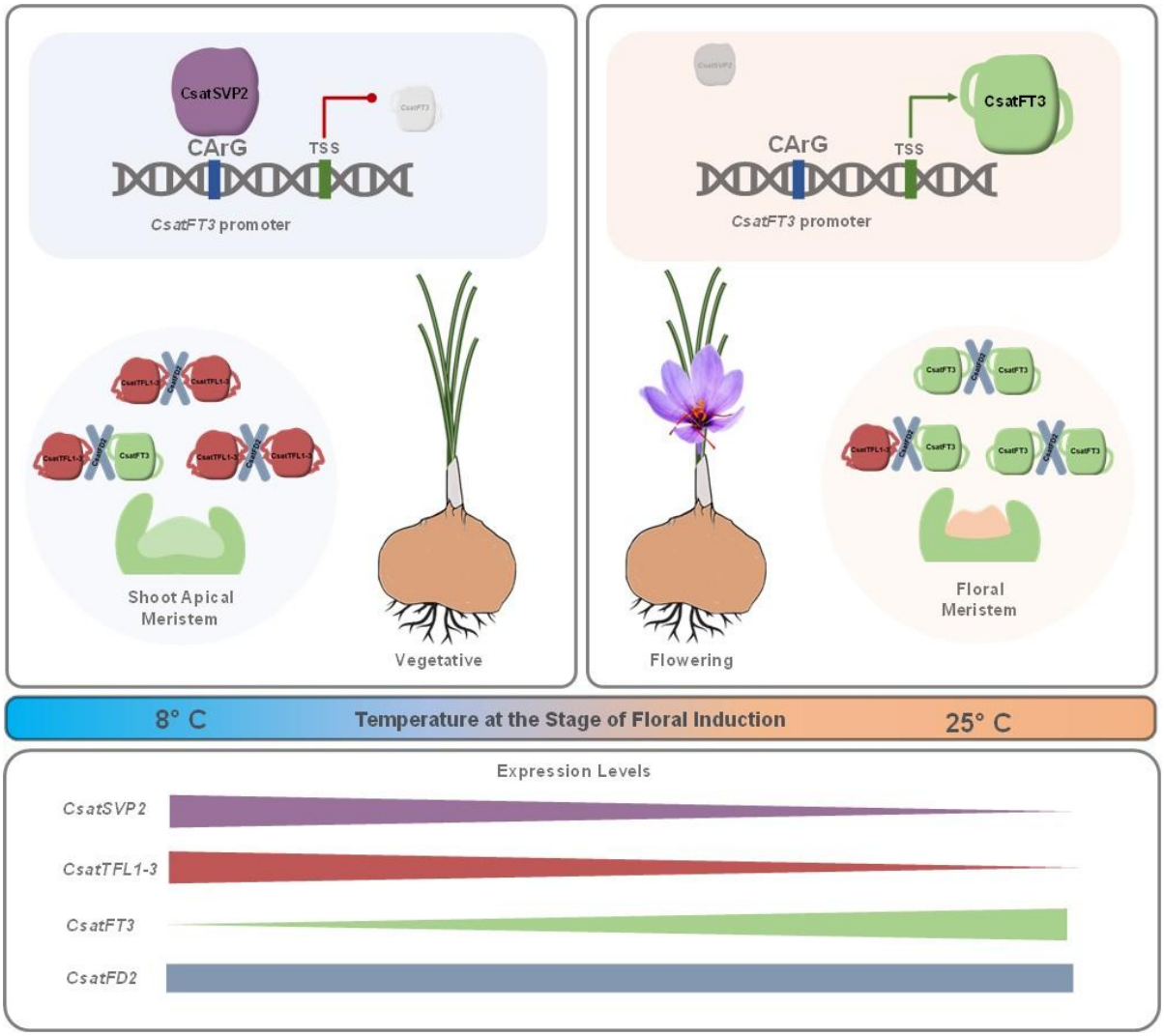

1043

1044

1045

1046

1047

1048

1049

1050

1051

1052

1053

1054

1055 ## References

1056 Abe, M., Kobayashi, Y., Yamamoto, S., Daimon, Y., Yamaguchi, A., Ikeda, Y., Ichinoki, H., Notaguchi, M.,
1057 Goto, K. and Araki, T. (2005) FD, a bZIP protein mediating signals from the floral pathway
1058 integrator FT at the shoot apex. *Science* **309**, 1052-1056.
1059 Ahrazem, O., Rubio-Moraga, A., Nebauer, S.G., Molina, R.V. and Gomez-Gomez, L. (2015) Saffron: Its
1060 Phytochemistry, Developmental Processes, and Biotechnological Prospects. *J Agric Food Chem*
1061 **63**, 8751-8764.
1062 Andrés, F. and Coupland, G. (2012) The genetic basis of flowering responses to seasonal cues. *Nature*
1063 *Reviews Genetics* **13**, 627-639.
1064 Balasubramanian, S., Sureshkumar, S., Lempe, J. and Weigel, D. (2006) Potent induction of Arabidopsis
1065 thaliana flowering by elevated growth temperature. *PLoS genetics* **2**, e106.
1066 Bellinazzo, F., Manders, I., Heidemann, B., Bolanos, M.A., Stouten, E., Busscher, J., Abarca, D., van der
1067 Wal, F., Dornelas, M.C. and Angenent, G.C. (2025) Differential growth and flowering capacity
1068 of tulip bulbs and the potential involvement of PHOSPHATIDYLETHANOLAMINE-BINDING
1069 PROTEINS (PEBPs). *Biology Direct* **20**, 29.
1070 Blázquez, M.A., Trénor, M. and Weigel, D. (2002) Independent control of gibberellin biosynthesis and
1071 flowering time by the circadian clock in Arabidopsis. *Plant Physiology* **130**, 1770-1775.
1072 Bowman, J.L., Smyth, D.R. and Meyerowitz, E.M. (2012) The ABC model of flower development: then
1073 and now. *Development* **139**, 4095-4098.
1074 Capovilla, G., Schmid, M. and Posé, D. (2015) Control of flowering by ambient temperature. *Journal of*
1075 *Experimental Botany* **66**, 59-69.
1076 Cardone, L., Castronuovo, D., Perniola, M., Cicco, N. and Candido, V. (2020) Saffron (Crocus sativus L.),
1077 the king of spices: An overview. *Scientia Horticulturae* **272**, 109560.
1078 Freytes, S.N., Canelo, M. and Cerdán, P.D. (2021) Regulation of flowering time: when and where?
1079 *Current Opinion in Plant Biology* **63**, 102049.
1080 Gu, X., Le, C., Wang, Y., Li, Z., Jiang, D., Wang, Y. and He, Y. (2013) Arabidopsis FLC clade members
1081 form flowering-repressor complexes coordinating responses to endogenous and
1082 environmental cues. *Nature Communications* **4**, 1947.
1083 Heide, O.M. (1977) Photoperiod and temperature interactions in growth and flowering of strawberry.
1084 *Physiologia Plantarum* **40**, 21-26.
1085 Hsu, C.-Y., Adams, J.P., Kim, H., No, K., Ma, C., Strauss, S.H., Drnevich, J., Vandervelde, L., Ellis, J.D. and
1086 Rice, B.M. (2011) FLOWERING LOCUS T duplication coordinates reproductive and vegetative
1087 growth in perennial poplar. *Proceedings of the National Academy of Sciences* **108**, 10756-
1088 10761.
1089 Hu, J., Liu, Y., Tang, X., Rao, H., Ren, C., Chen, J., Wu, Q., Jiang, Y., Geng, F. and Pei, J. (2020)
1090 Transcriptome profiling of the flowering transition in saffron (Crocus sativus L.). *Scientific*
1091 *Reports* **10**, 9680.
1092 Jefferson, R.A., Kavanagh, T.A. and Bevan, M.W. (1987) GUS fusions: beta-glucuronidase as a sensitive
1093 and versatile gene fusion marker in higher plants. *Embo j* **6**, 3901-3907.
1094 Jin, S. and Ahn, J.H. (2021) Regulation of flowering time by ambient temperature: repressing the
1095 repressors and activating the activators. *New Phytologist* **230**, 938-942.
1096 Jin, S., Nasim, Z., Susila, H. and Ahn, J.H. (2021) Evolution and functional diversification of FLOWERING
1097 LOCUS T/TERMINAL FLOWER 1 family genes in plants. *Seminars in Cell & Developmental*
1098 *Biology* **109**, 20-30.
1099 Jing, S., Jiang, P., Sun, X., Yu, L., Wang, E., Qin, J., Zhang, F., Prat, S. and Song, B. (2023) Long-distance
1100 control of potato storage organ formation by SELF PRUNING 3D and FLOWERING LOCUS T-like
1101 1. *Plant communications* **4**.
1102 Jose-Santhi, J., Sheikh, F.R., Kalia, D. and Singh, R.K. (2023) Sugar metabolism mediates temperature-
1103 dependent flowering induction in saffron (Crocus sativus L.). *Environmental and Experimental*
1104 *Botany* **206**, 105150.

1105 Kalia, D., Jose-Santhi, J., Kumar, R. and Singh, R.K. (2022) Analysis of PEBP Genes in Saffron Identifies
1106 a Flowering Locus T Homologue Involved in Flowering Regulation. *Journal of Plant Growth*
1107 *Regulation*, 1-20.
1108 Kalia, D., Jose-Santhi, J., Kumar, R. and Singh, R.K. (2023) Analysis of PEBP genes in saffron identifies a
1109 flowering locus T homologue involved in flowering regulation. *Journal of Plant Growth*
1110 *Regulation* **42**, 2486-2505.
1111 Kalia, D., Jose-Santhi, J., Sheikh, F.R., Singh, D. and Singh, R.K. (2024) Tobacco rattle virus-based virus-
1112 induced gene silencing (VIGS) as an aid for functional genomics in Saffron (Crocus sativus L.).
1113 *Physiol Mol Biol Plants* **30**, 749-755.
1114 Khodorova, N.V. and Boitel-Conti, M. (2013) The role of temperature in the growth and flowering of
1115 geophytes. *Plants* **2**, 699-711.
1116 Khosa, J., Bellinazzo, F., Kamenetsky Goldstein, R., Macknight, R. and Immink, R.G.H. (2021)
1117 PHOSPHATIDYLETHANOLAMINE-BINDING PROTEINS: the conductors of dual reproduction in
1118 plants with vegetative storage organs. *Journal of Experimental Botany* **72**, 2845-2856.
1119 Kinoshita, A. and Richter, R. (2020) Genetic and molecular basis of floral induction in Arabidopsis
1120 thaliana. *Journal of Experimental Botany* **71**, 2490-2504.
1121 Lee, C., Kim, S.J., Jin, S., Susila, H., Youn, G., Nasim, Z., Alavilli, H., Chung, K.S., Yoo, S.J. and Ahn, J.H.
1122 (2019) Genetic interactions reveal the antagonistic roles of FT/TSF and TFL1 in the
1123 determination of inflorescence meristem identity in Arabidopsis. *The Plant Journal* **99**, 452-
1124 464.
1125 Lee, J.H., Ryu, H.-S., Chung, K.S., Posé, D., Kim, S., Schmid, M. and Ahn, J.H. (2013a) Regulation of
1126 Temperature-Responsive Flowering by MADS-Box Transcription Factor Repressors. *Science*
1127 **342**, 628-632.
1128 Lee, J.H., Yoo, S.J., Park, S.H., Hwang, I., Lee, J.S. and Ahn, J.H. (2007) Role of SVP in the control of
1129 flowering time by ambient temperature in Arabidopsis. *Genes & development* **21**, 397-402.
1130 Lee, R., Baldwin, S., Kenel, F., McCallum, J. and Macknight, R. (2013b) FLOWERING LOCUS T genes
1131 control onion bulb formation and flowering. *Nat Commun* **4**, 2884.
1132 Leeggangers, H.A., Nijveen, H., Bigas, J.N., Hilhorst, H.W. and Immink, R.G. (2017a) Molecular
1133 regulation of temperature-dependent floral induction in Tulipa gesneriana. *Plant physiology*
1134 **173**, 1904-1919.
1135 Leeggangers, H.A., Nijveen, H., Bigas, J.N., Hilhorst, H.W. and Immink, R.G. (2017b) Molecular
1136 Regulation of Temperature-Dependent Floral Induction in Tulipa gesneriana. *Plant Physiol*
1137 **173**, 1904-1919.
1138 Li, X.-F., Wu, W.-T., Zhang, X.-P., Qiu, Y., Zhang, W., Li, R., Xu, J., Sun, Y., Wang, Y. and Xu, L. (2015)
1139 Narcissus tazetta SVP-like gene NSVP1 affects flower development in Arabidopsis. *Journal of*
1140 *Plant Physiology* **173**, 89-96.
1141 Lu, J., Qu, L., Xing, G., Liu, Z., Lu, X. and Han, X. (2023) Genome-Wide Identification and Expression
1142 Analysis of the MADS Gene Family in Tulips (Tulipa gesneriana). *Genes (Basel)* **14**.
1143 Molina, R., Valero, M., Navarro, Y., Guardiola, J. and Garcia-Luis, A. (2005a) Temperature effects on
1144 flower formation in saffron (Crocus sativus L.). *Scientia horticulturae* **103**, 361-379.
1145 Molina, R.V., M., V., Y., N., A., G.-L. and and Guardiola, J.L. (2005b) Low temperature storage of corms
1146 extends the flowering season of saffron (Crocus sativus L.). *The Journal of Horticultural Science*
1147 *and Biotechnology* **80**, 319-326.
1148 Nakano, Y., Higuchi, Y., Sumitomo, K. and Hisamatsu, T. (2013) Flowering retardation by high
1149 temperature in chrysanthemums: involvement of FLOWERING LOCUS T-like 3 gene
1150 repression. *Journal of Experimental Botany* **64**, 909-920.
1151 Navarro, C., Abelenda, J.A., Cruz-Oró, E., Cuéllar, C.A., Tamaki, S., Silva, J., Shimamoto, K. and Prat, S.
1152 (2011) Control of flowering and storage organ formation in potato by FLOWERING LOCUS T.
1153 *Nature* **478**, 119-122.

1154 Noy-Porat, T., Cohen, D., Mathew, D., Eshel, A., Kamenetsky, R. and Flaishman, M.A. (2013) Turned on
1155 by heat: differential expression of FT and LFY-like genes in Narcissus tazetta during floral
1156 transition. *Journal of experimental botany* **64**, 3273-3284.
1157 Oda, A., Narumi, T., Li, T., Kando, T., Higuchi, Y., Sumitomo, K., Fukai, S. and Hisamatsu, T. (2012)
1158 CsFTL3, a chrysanthemum FLOWERING LOCUS T-like gene, is a key regulator of photoperiodic
1159 flowering in chrysanthemums. *Journal of Experimental Botany* **63**, 1461-1477.
1160 Pin, P.A., Benlloch, R., Bonnet, D., Wremerth-Weich, E., Kraft, T., Gielen, J.J. and Nilsson, O. (2010) An
1161 antagonistic pair of FT homologs mediates the control of flowering time in sugar beet. *Science*
1162 **330**, 1397-1400.
1163 Putterill, J., Laurie, R. and Macknight, R. (2004) It's time to flower: the genetic control of flowering
1164 time. *BioEssays* **26**, 363-373.
1165 Pyo, Y., Park, S., Xi, Y. and Sung, S. (2014) Regulation of flowering by vernalisation in Arabidopsis. In:
1166 *Advances in botanical research* pp. 29-61. Elsevier.
1167 Renau-Morata, B., Nebauer, S.G., García-Carpintero, V., Cañizares, J., Gómez Minguet, E., de los
1168 Mozos, M. and Molina, R.V. (2021) Flower induction and development in saffron: Timing and
1169 hormone signalling pathways. *Industrial Crops and Products* **164**, 113370.
1170 Simon, R., Igeño, M.I. and Coupland, G. (1996) Activation of floral meristem identity genes in
1171 Arabidopsis. *Nature* **384**, 59-62.
1172 Singh, D., Sharma, S., Jose-Santhi, J., Kalia, D. and Singh, R.K. (2023) Hormones regulate the flowering
1173 process in saffron differently depending on the developmental stage. *Front Plant Sci* **14**,
1174 1107172.
1175 Srikanth, A. and Schmid, M. (2011) Regulation of flowering time: all roads lead to Rome. *Cellular and*
1176 *molecular life sciences* **68**, 2013-2037.
1177 Strasser, B., Alvarez, M.J., Califano, A. and Cerdán, P.D. (2009) A complementary role for ELF3 and TFL1
1178 in the regulation of flowering time by ambient temperature. *The Plant Journal* **58**, 629-640.
1179 Sureshkumar, S., Dent, C., Seleznev, A., Tasset, C. and Balasubramanian, S. (2016) Nonsense-mediated
1180 mRNA decay modulates FLM-dependent thermosensory flowering response in Arabidopsis.
1181 *Nat Plants* **2**, 16055.
1182 Taoka, K.-i., Ohki, I., Tsuji, H., Kojima, C. and Shimamoto, K. (2013) Structure and function of florigen
1183 and the receptor complex. *Trends in plant science* **18**, 287-294.
1184 Tsaftaris, A., Pasentsis, K. and Argiriou, A. (2013) Cloning and Characterization of FLOWERING LOCUS
1185 T-Like Genes from the Perennial Geophyte Saffron Crocus (Crocus sativus). *Plant Mol. Biol.*
1186 *Report.* **31**, 1558–1568.
1187 Tsuji, H., Nakamura, H., Taoka, K. and Shimamoto, K. (2013) Functional diversification of FD
1188 transcription factors in rice, components of florigen activation complexes. *Plant Cell Physiol*
1189 **54**, 385-397.
1190 Turck, F., Fornara, F. and Coupland, G. (2008) Regulation and identity of florigen: FLOWERING LOCUS
1191 T moves center stage. *Annu. Rev. Plant Biol.* **59**, 573-594.
1192 Tylewicz, S., Tsuji, H., Miskolczi, P., Petterle, A., Azeez, A., Jonsson, K., Shimamoto, K. and Bhalerao,
1193 R.P. (2015) Dual role of tree florigen activation complex component FD in photoperiodic
1194 growth control and adaptive response pathways. *Proceedings of the National Academy of*
1195 *Sciences* **112**, 3140-3145.
1196 Wang, Z., Li, X., Xu, J., Yang, Z. and Zhang, Y. (2021) Effects of ambient temperature on flower initiation
1197 and flowering in saffron (Crocus sativus L.). *Scientia Horticulturae* **279**, 109859.
1198 Wickland, D.P. and Hanzawa, Y. (2015) The FLOWERING LOCUS T/TERMINAL FLOWER 1 gene family:
1199 functional evolution and molecular mechanisms. *Molecular plant* **8**, 983-997.
1200 Wigge, Philip A. (2011) FT, A Mobile Developmental Signal in Plants. *Current Biology* **21**, R374-R378.
1201 Wigge, P.A., Kim, M.C., Jaeger, K.E., Busch, W., Schmid, M., Lohmann, J.U. and Weigel, D. (2005)
1202 Integration of spatial and temporal information during floral induction in Arabidopsis. *Science*
1203 **309**, 1056-1059.

1204 Wu, X., Ling, W., Pan, Y., Yang, Z., Ma, J., Yang, Y., Xiang, W., Zhou, L., Sun, M., Chen, J., Chen, H., Zheng,
1205 S., Zeng, J. and Li, Y. (2024) Functional analysis of a lily SHORT VEGETATIVE PHASE ortholog in
1206 flowering transition and floral development. *Plant Physiology and Biochemistry* **206**, 108287.
1207 Wu, Y.-M., Ma, Y.-J., Wang, M., Zhou, H., Gan, Z.-M., Zeng, R.-F., Ye, L.-X., Zhou, J.-J., Zhang, J.-Z. and
1208 Hu, C.-G. (2022) Mobility of FLOWERING LOCUS T protein as a systemic signal in trifoliate
1209 orange and its low accumulation in grafted juvenile scions. *Horticulture Research* **9**.
1210 Xue, W., Shi, J., Li, Z., Zhang, Y., Tang, M., Du, X., An, Z., Chen, H., Yang, D. and Li, X. (2025) CmFDa-
1211 mediated epigenetic regulation of flowering in chrysanthemum. *Plant Biotechnology Journal*.
1212 Yan, X., Cao, Q.-Z., He, H.-B., Wang, L.-J. and Jia, G.-X. (2021) Functional analysis and expression
1213 patterns of members of the FLOWERING LOCUS T (FT) gene family in Lilium. *Plant Physiology*
1214 *and Biochemistry* **163**, 250-260.
1215 Zhu, Y., Klasfeld, S., Jeong, C.W., Jin, R., Goto, K., Yamaguchi, N. and Wagner, D. (2020) TERMINAL
1216 FLOWER 1-FD complex target genes and competition with FLOWERING LOCUS T. *Nature*
1217 *communications* **11**, 5118.
1218 Zik, M. and Irish, V.F. (2003) Global identification of target genes regulated by APETALA3 and
1219 PISTILLATA floral homeotic gene action. *The Plant Cell* **15**, 207-222.

1220